Electronic Supplementary Information

Potentiostatically Controlled Olefin Metathesis

Guillermo Ahumada,[†,‡] Yeonkyeong Ryu[†,‡] and Christopher W. Bielawski[†,‡,#,*]

† Center for Multidimensional Carbon Materials (CMCM), Institute for Basic Science (IBS), Ulsan 44919 (Republic of Korea)

‡ Department of Chemistry, Ulsan National Institute of Science and Technology (UNIST), Ulsan 44919 (Republic of Korea)

Department of Energy Engineering, Ulsan National Institute of Science and Technology (UNIST), Ulsan 44919 (Republic of Korea)

* Correspondence: bielawski@unist.ac.kr; Tel.: +82-52-217-2952

Table of Contents

1. General considerations

All procedures were performed in a nitrogen-filled glove box using oven-dried glassware unless otherwise noted. Solvents were dried and degassed by a Vacuum Atmospheres Company solvent purification system and stored over 4 Å molecular sieves in a nitrogen-filled glove box. Reagents were purchased from commercial sources and used without further purification unless otherwise noted. Complex **1** was synthesized according to a procedure reported in the literature.[1] ^{1}H NMR spectra were recorded in chloroform-d_1 (^{1}H: 7.26 ppm) using a Bruker 400 MHz spectrometer. Size exclusion chromatography (SEC) was performed on a Malvern GPCmax solvent/sample module equipped with a refractive index detector. THF was used as the eluent at a flow rate of 0.8 mL min^{-1}. Molecular weights are reported against poly(styrene) standards.

1.1 General procedure: cyclic voltammetry and differential pulse voltammetry

Cyclic voltammetry was conducted using a CH Instruments Electrochemical Workstation (series 680) and a three-electrode configuration, where a platinum disk (diameter: 1.6 mm) was used as a working electrode, a platinum coil was used as a counter electrode and a non-aqueous Ag/Ag$^+$ (acetonitrile) was used as a reference electrode. Unless otherwise noted, all potentials were determined at a scan rate of 100 mV·s^{-1} and referenced to a saturated calomel electrode (SCE) by shifting Fc/Fc$^+$ to +0.18 V.[2] After each experiment, the disk electrode was polished and the platinum coil was washed with aqua regia followed excess water and then flame dried. The reference electrode was washed with dichloromethane after each experiment and calibrated in 10 mL of dichloromethane containing ferrocene (1×10^{-3} M) and $TBAPF_6$ (0.01 M). Differential pulse voltammetry was conducted under similar conditions using a pulse range of 0.25 mV/s.

1.2 General procedure: bulk electrolysis

Bulk electrolysis experiments were performed in a three-chamber electrochemical cell (Figure S1) that was obtained from Adams & Chittenden Scientific Glass (model No. 945059). Each compartment was divided by a P5 glass frit to maintain separation between the counter electrode solution and the working electrode solution. The separation prevents the soluble products produced in the counter electrode from reacting at the working electrode. Vigorous stirring was required to

achieve an optimal current response. The cell was equipped with a platinum mesh working electrode (1.6 g), a platinum coil as a counter electrode, and a non-aqueous (acetonitrile) Ag/Ag^+ reference electrode . Measurements were performed in dry dichloromethane with 0.01 M $TBAPF_6$ as electrolyte. Unless otherwise noted, all potentials are referenced to a saturated calomel electrode (SCE) by shifting Fc/Fc^+ to +0.18 V.[2] The measurements were made using a CH Instruments Electrochemical Workstation (series 680). After each experiment, the working (mesh) and counter (coil) platinum electrodes were washed with aqua regia followed by excess water and then flame dried. The reference electrode was washed with dichloromethane after each experiment and calibrated in 10 mL of dichloromethane containing ferrocene (1×10^{-3} M) and $TBAPF_6$ (0.01 M).

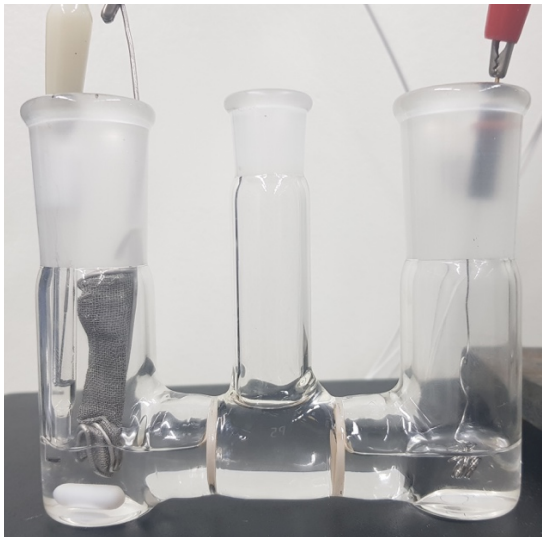

Figure S1 A photograph of the three-chamber cell that was used to conduct the bulk electrolysis experiments. The left chamber contains a Pt mesh working electrode and a Ag/Ag^+ (acetonitrile) reference electrode. The right chamber contains a Pt coil as a counter electrode.

1.3 General procedure: generation of $\mathbf{1}_{red}$

To generate $\mathbf{1}_{red}$, the cell was loaded with a stir bar and a dichloromethane solution of **1** ($[\mathbf{1}]_0 = 0.5$ mM) containing tetrabutylammonium hexafluorophosphate ($[TBAPF_6]_0 = 0.01$ mM) as electrolyte. A fixed potential of -0.95 V was then applied for approximately 20 min. CV of the resulting solution revealed signals that were consistent with the NQ|NQ- redox couples of the starting material (Figure S3).

1.4 General procedure: potentiostatically-controlled RCM and ROMP

Each chamber of a three-chamber cell was charged with 10 mL of dichloromethane, $TBAPF_6$ (0.01 M) as electrolyte, and 1,3,5-trimethoxybenzene (TMB; 0.05 M) as an internal standard. The chamber containing the working and reference electrodes was loaded with catalyst (0.5 mM) and substrate (0.05 M). Aliquots were periodically removed from the reaction vessel, diluted with THF, and then analyzed with an Agilent 6850 gas chromatograph.

1.5 Kinetic analyses

The ring-closing metathesis of DDM or the ring-opening metathesis polymerization of COD may be represented as:

$$A + B \longrightarrow C$$

Assuming that the substrate (A) will always be present in a large excess compared to the catalyst (B) and no side reactions, the following rate law applies:

$$\frac{d[C]}{dt} = k'[A][B]_0 = k[A]$$

The integrated form of the above equation may be re-written as:

$$\ln[A] = \ln[A]_0 - kt$$

Thus, plotting -ln[*A*] versus *t* should afford a linear relationship where the rate constant *k* is equal to the slope of the line.

2. Electrochemical data

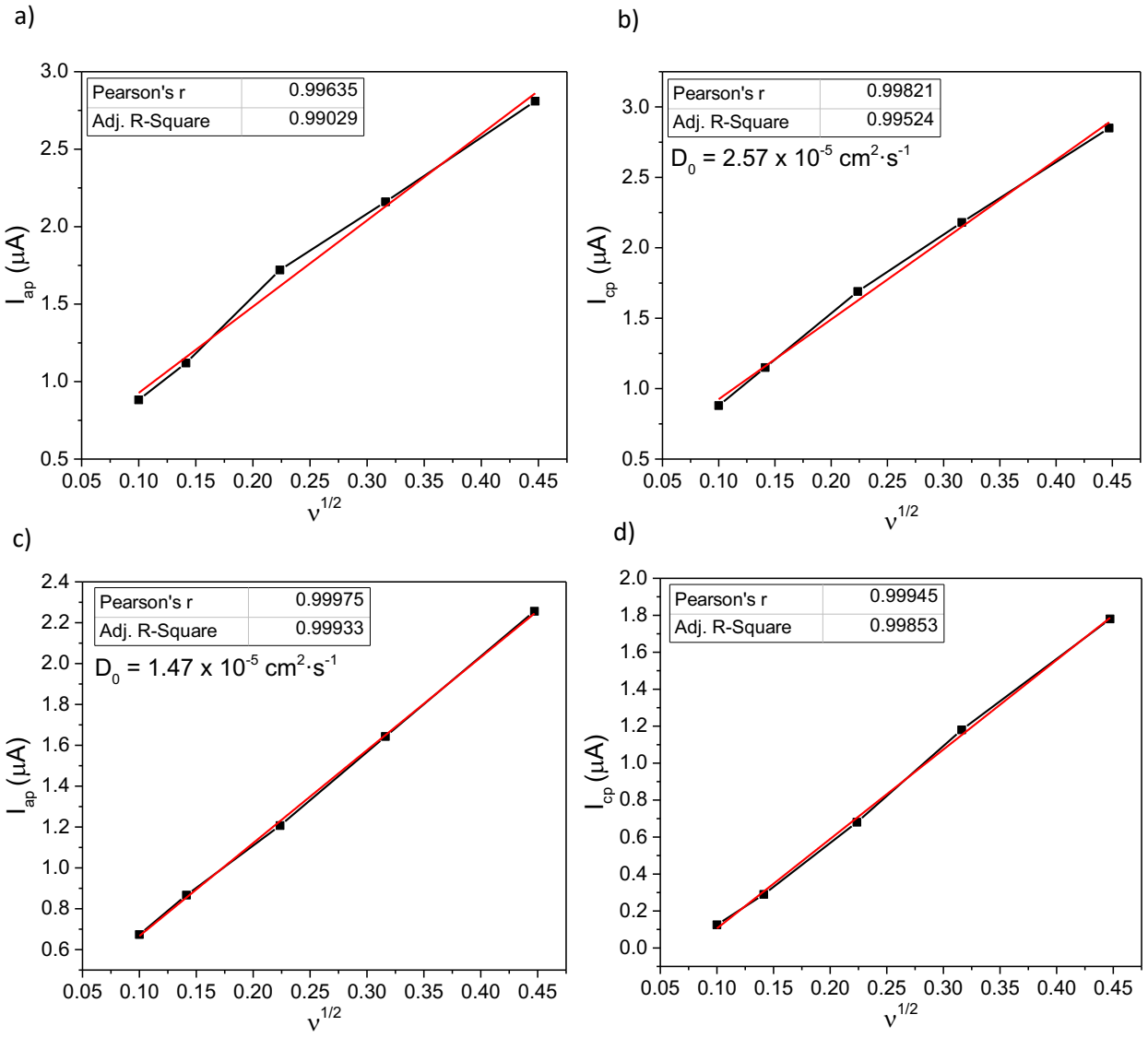

Figure S2 Plots of the (a) anodic and (b) cathodic peak currents vs. the square root of the scan rate for the process assigned to the NQ|NQ^- redox couple for **1**. Plots of the (c) anodic and (d) cathodic peak currents vs. the square root of the scan rate for the process assigned to the NQ^-|NQ redox couple for $\mathbf{1}_{red}$ as generated by bulk electrolysis (Figure S3). Conditions: $[\mathbf{1}]_0$ = 0.5 mM, $[TBAPF_6]_0$ = 0.01 M, CH_2Cl_2.

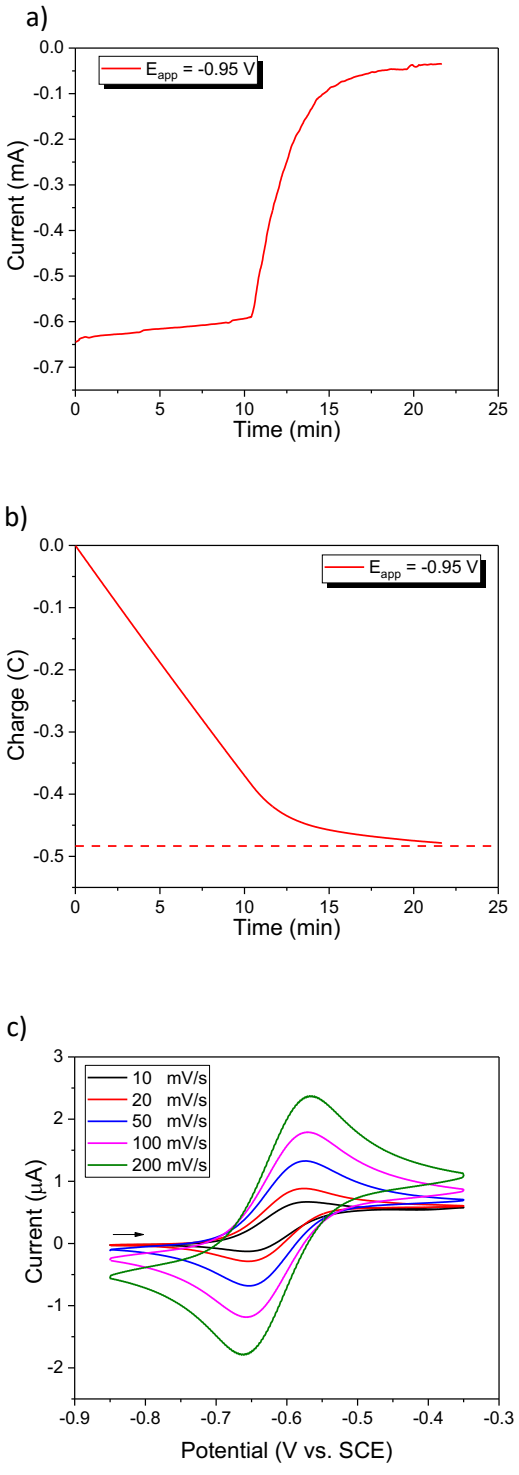

Figure S3 (a) Plot of current vs. time as recorded after applying a potential of -0.95 V to a solution of **1**. (b) Corresponding plot of charge vs. time. (c) CV of $\mathbf{1}_{red}$ as recorded at different scan rates (indicated). Conditions: $[\mathbf{1}]_0$ = 0.5 mM, $[TBAPF_6]_0$ = 0.01 M, CH_2Cl_2.

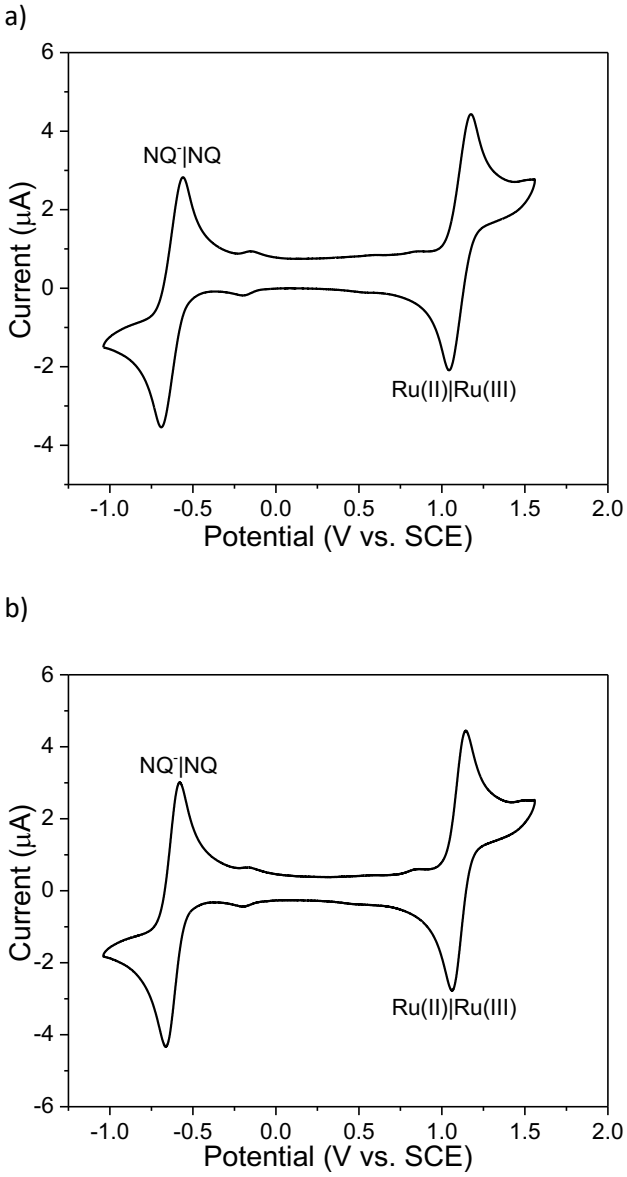

Figure S4 (a) Cyclic voltammetry data recorded after reducing **1** by applying a potential of -0.95 V for 20 min. (b) Cyclic voltammetry data recorded after oxidizing the reduced catalyst ($\mathbf{1}_{red}$) by applying a potential of +0.34 V for 18 min. Conditions: $[\mathbf{1}]_0$ = 0.5 mM, $[TBAPF_6]_0$ = 0.01 M, CH_2Cl_2.

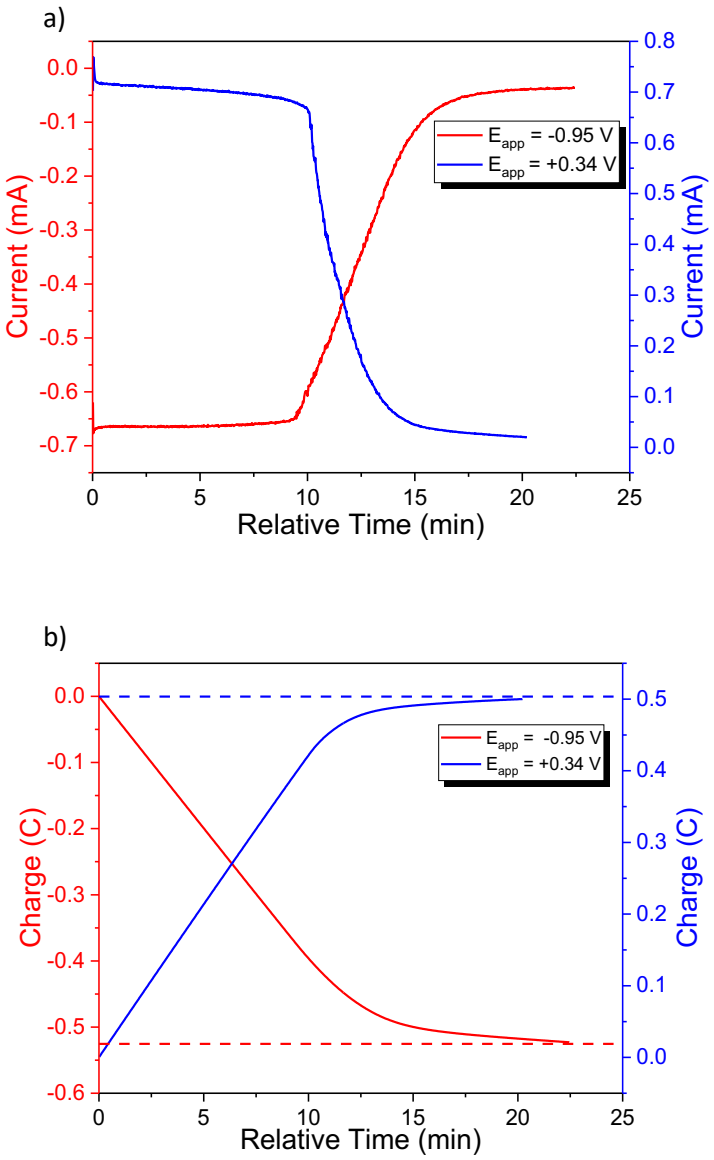

Figure S5 (a) Plots of current vs. relative time as recorded after one reduction-oxidation cycle, which was achieved by applying a potential of -0.95 V (red) followed by +0.34 V (blue) to a solution containing **1** or $\mathbf{1}_{red}$. Note: the data recorded under oxidizing conditions (blue) were obtained after the complex was reduced (red). (b) Corresponding plots of charge vs. relative time. Conditions: $[\mathbf{1}]_0$ = 0.5 mM, $[TBAPF_6]_0$ = 0.01 M, CH_2Cl_2.

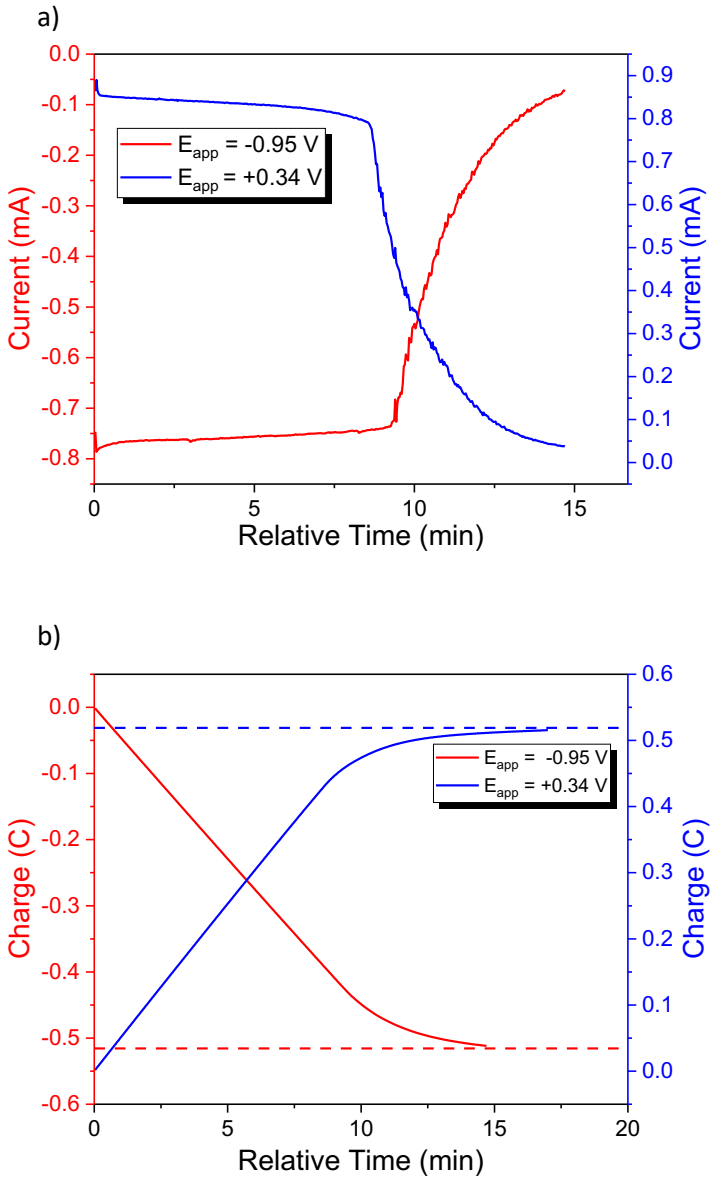

Figure S6 (a) Plots of current vs. relative time as recorded after two reduction-oxidation cycles, which was achieved by applying a potential of -0.95 V (red) followed by +0.34 V (blue) to a solution containing **1** or $\mathbf{1}_{red}$ (twice). Note: the data recorded under oxidizing conditions (blue) were obtained after the complex was reduced (red). (b) Corresponding plots of charge vs. relative time. Conditions: $[\mathbf{1}]_0 = 0.5$ mM, $[TBAPF_6]_0 = 0.01$ M, CH_2Cl_2.

Table S1 Summary of charges recovered over multiple bulk electrolysis cycles.[a]

Cycle	Reduction (C)	Oxidation (C)	Recovery (%)
1	-0.5290	0.5088	96
2	-0.5230	0.5001	96
3	-0.5118	0.5155	99
Average	-0.5213	0.5081	97

[a] Conditions: $[\mathbf{1}]_0$ = 0.5 mM, $[TBAPF_6]_0$ = 0.01 M, CH_2Cl_2.

3. Bulk electrolysis control experiments

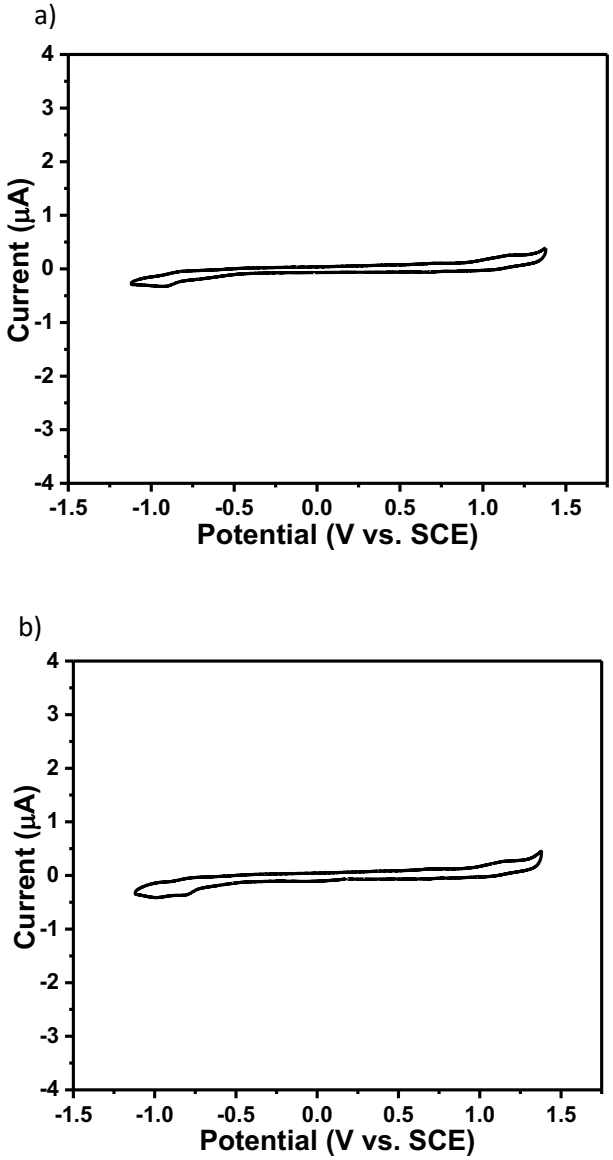

Figure S7 (a) Cyclic voltammetry data that were recorded for a CH_2Cl_2 solution containing DDM, TMB and $TBAPF_6$ (no catalyst). (b) Cyclic voltammetry data that were recorded after the solution described in (a) was subjected to a full electrolysis cycle (reduction and oxidation), which was conducted in the following order: (1) a potential of -0.95 V was applied for 20 min; (2) the potential was removed; (3) the mixture was stirred for 30 min; and (4) a potential of +0.34 V was applied for 20 min. Conditions: $[DDM]_0$ = 0.05 M, $[TMB]_0$ = 0.05 M, $[TBAPF_6]_0$ = 0.01 M, CH_2Cl_2.

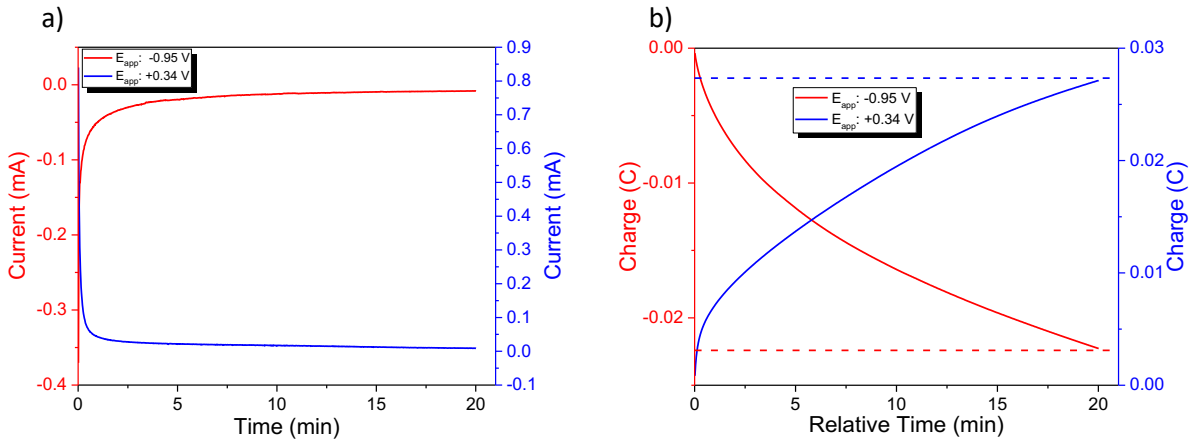

Figure S8 (a) Plots of current vs. relative time upon the application of a potential of -0.95 V (red) or +0.34 V (blue) to a solution containing DDM, TMB and $TBAPF_6$ (no catalyst). Note: the data shown under oxidizing conditions (blue) were recorded 30 min after the reduction process was complete (red). (b) Corresponding plots of charge vs. relative time. Conditions: $[DDM]_0 = 0.05$ M, $[TMB]_0 = 0.05$ M, $[TBAPF_6]_0 = 0.01$ M, CH_2Cl_2.

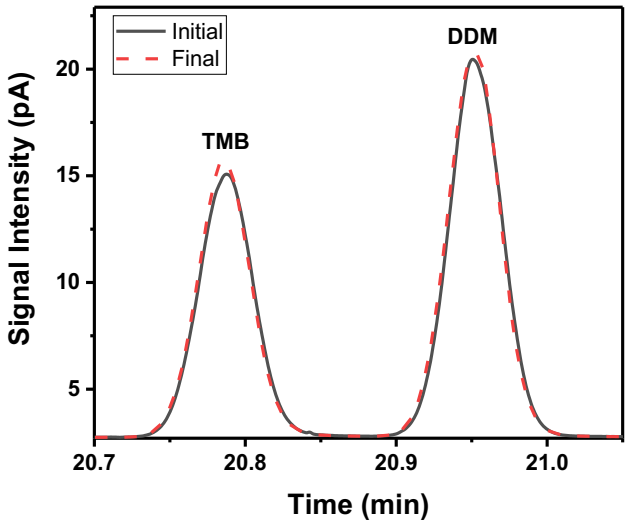

Figure S9 GC data that were recorded at the beginning and at the end of the bulk electrolysis control experiment which was performed in the absence of catalyst. Conditions: $[DDM]_0 = 0.05$ M, $[TMB]_0 = 0.05$ M, $[TBAPF_6]_0 = 0.01$ M, CH_2Cl_2.

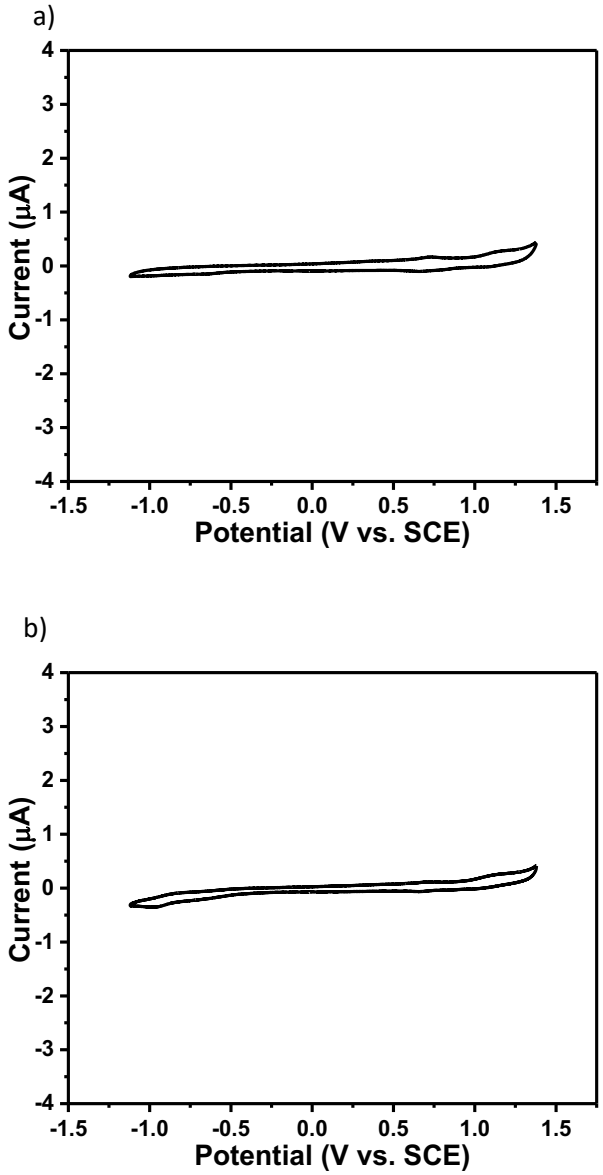

Figure S10 (a) Cyclic voltammetry data that were recorded for a CH_2Cl_2 solution containing COD, TMB and $TBAPF_6$ (no catalyst). (b) Cyclic voltammetry data that were recorded after the solution described in (a) was subjected to a full electrolysis cycle (reduction and oxidation), which was conducted in the following order: (1) a potential of -0.95 V was applied for 20 min; (2) the potential was removed; (3) the mixture was stirred for 30 min; and (4) a potential of +0.34 V was applied for 20 min. Conditions: $[COD]_0$ = 0.05 M, $[TMB]_0$ = 0.05 M, $[TBAPF_6]_0$ = 0.01 M, CH_2Cl_2.

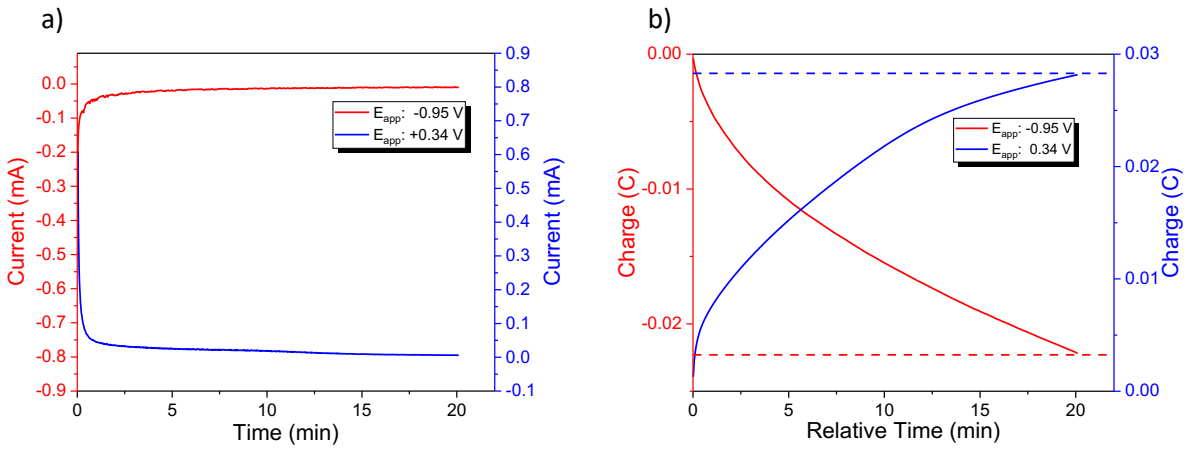

Figure S11 (a) Plots of current vs. relative time upon the application of a potential of -0.95 V (red) or +0.34 V (blue) to a solution containing COD, TMB and $TBAPF_6$ (no catalyst). Note: the data shown under oxidizing conditions (blue) were recorded 30 min after the reduction process was complete (red). (b) Corresponding plots of charge vs. relative time. Conditions: $[COD]_0 = 0.05$ M, $[TMB]_0 = 0.05$ M, $[TBAPF_6]_0 = 0.01$ M, CH_2Cl_2.

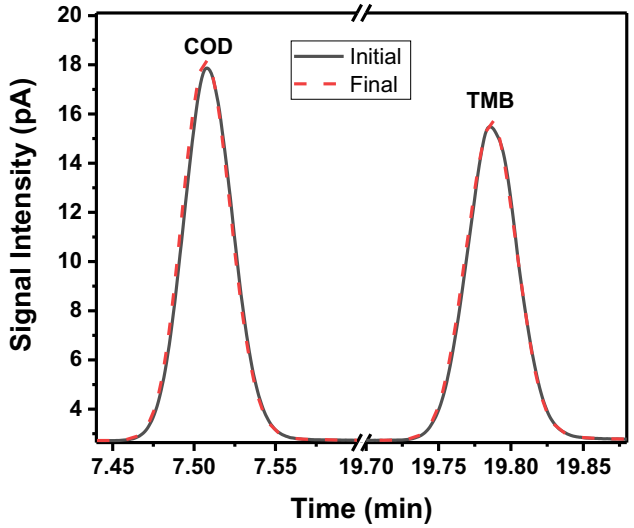

Figure S12 GC data that were recorded at the beginning and at the end of the bulk electrolysis control experiment which was performed in the absence of catalyst. Conditions: $[COD]_0 = 0.05$ M, $[TMB]_0 = 0.05$ M, $[TBAPF_6]_0 = 0.01$ M, CH_2Cl_2.

4. Potentiostatically-controlled RCM data

a)

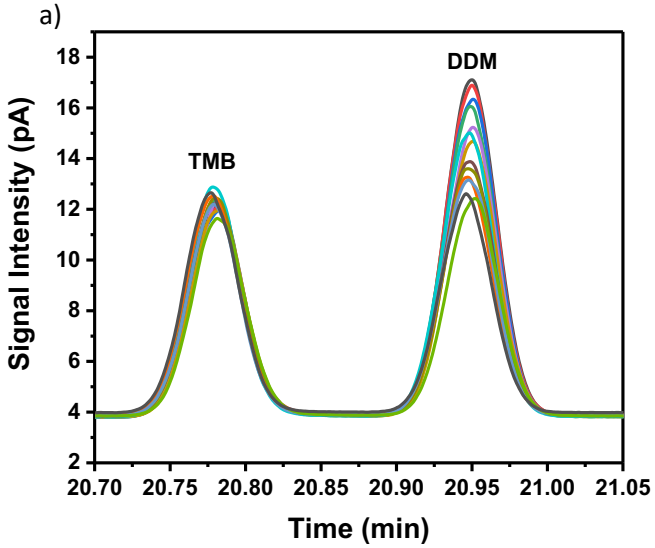

b)

t (min)	[DDM]/[TMB]	Conv. (%)
0	1.60	0
10	1.51	5.6
20	1.48	7.5
30	1.42	11.3
40	1.36	15.0
50	1.30	18.8
60	1.28	20.0
70	1.17	27.9
80	1.10	31.3
90	1.06	33.8
100	1.01	36.9
110	0.96	40.0
120	0.91	43.1

c)

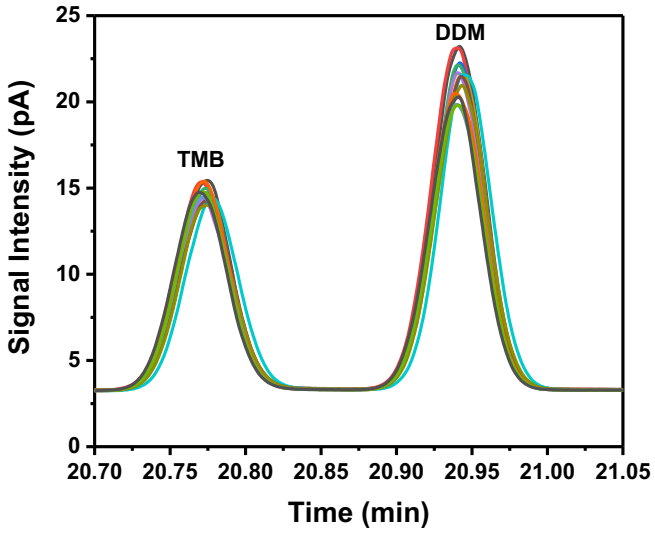

d)

t (min)	[DDM]/[TMB]	Conv. (%)
0	1.60	0
10	1.52	5.0
20	1.52	5.0
30	1.51	5.6
40	1.50	6.3
50	1.48	7.5
60	1.46	8.8
70	1.46	8.8
80	1.46	8.8
90	1.44	10.0
100	1.42	11.3
110	1.42	11.3
120	1.40	12.5

Figure S13 (a) Representative GC data recorded over time for the RCM of DDM using **1** as the catalyst. (b) Summary of the signal integral ratios for the data shown in panel (a) and the corresponding substrate conversions as a function of time. (c) Representative GC data recorded over time for the RCM of DDM using $\mathbf{1}_{red}$ as the catalyst. (d) Summary of the signal integral ratios for the data shown in panel (c) and the corresponding substrate conversions as a function of time. Conditions: $[DDM]_0 = 0.05$ M, $[\mathbf{1}]_0$ or $[\mathbf{1}_{red}]_0 = 0.5$ mM, $[TBAPF_6]_0 = 0.01$ M, $[TMB]_0 = 0.05$ M, CH_2Cl_2.

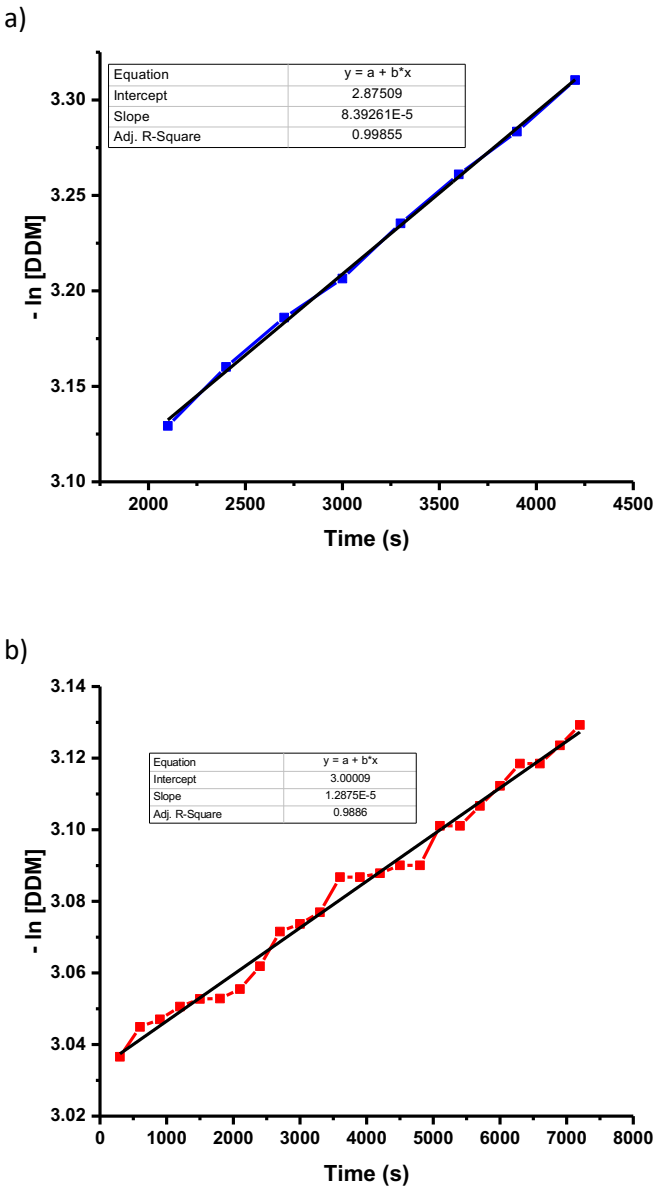

Figure S14 (a) Plot of –ln [DDM] vs. time using **1** as the catalyst (■). (b) Plot of –ln [DDM] vs time using $\mathbf{1_{red}}$ as the catalyst (■) (Figure S15). Conditions: $[DDM]_0 = 0.05$ M, $[\mathbf{1}]_0$ or $[\mathbf{1_{red}}]_0 = 0.5$ mM, $[TBAPF_6]_0 = 0.01$ M, $[TMB]_0 = 0.05$ M, CH_2Cl_2.

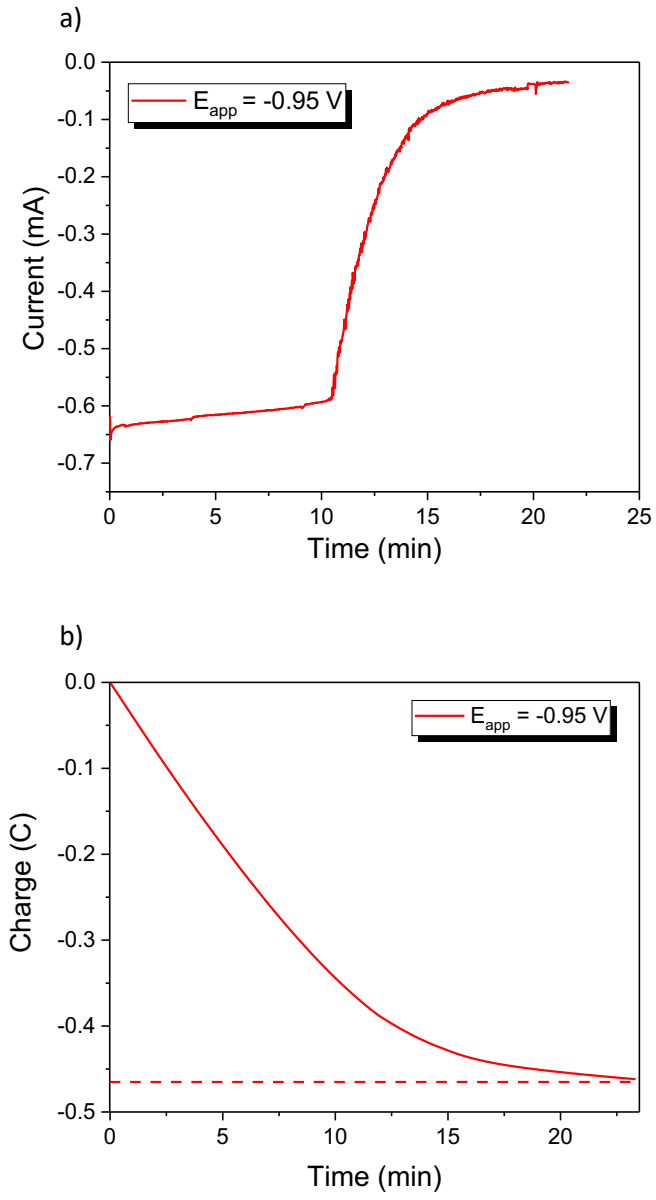

Figure S15 (a) Plot of current vs. time as recorded after applying a potential of -0.95 V to a solution of **1** and before the addition of DDM (Figure S14b). (b) Corresponding charge vs. time. Conditions: $[\mathbf{1}]_0$ = 0.5 mM, $[TBAPF_6]_0$ = 0.01 M, CH_2Cl_2.

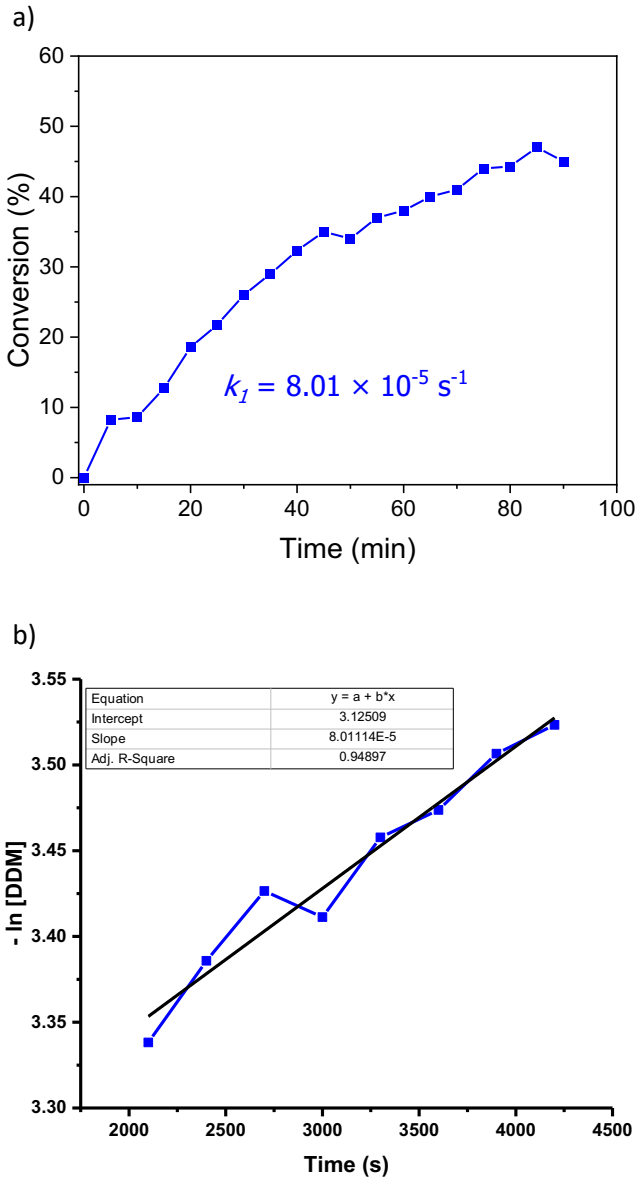

Figure S16 (a) Plot of conversion of DDM to its ring-closed product vs. time as catalyzed with **1** (■) after it was subjected to a reduction-oxidation cycle (Figure S17). (b) Corresponding plot of – ln [DDM] vs. time. Conditions: $[DDM]_0$ = 0.05 M, $[\mathbf{1}]_0$ = 0.5 mM, $[TBAPF_6]_0$ = 0.01 M, $[TMB]_0$ = 0.05 M, CH_2Cl_2.

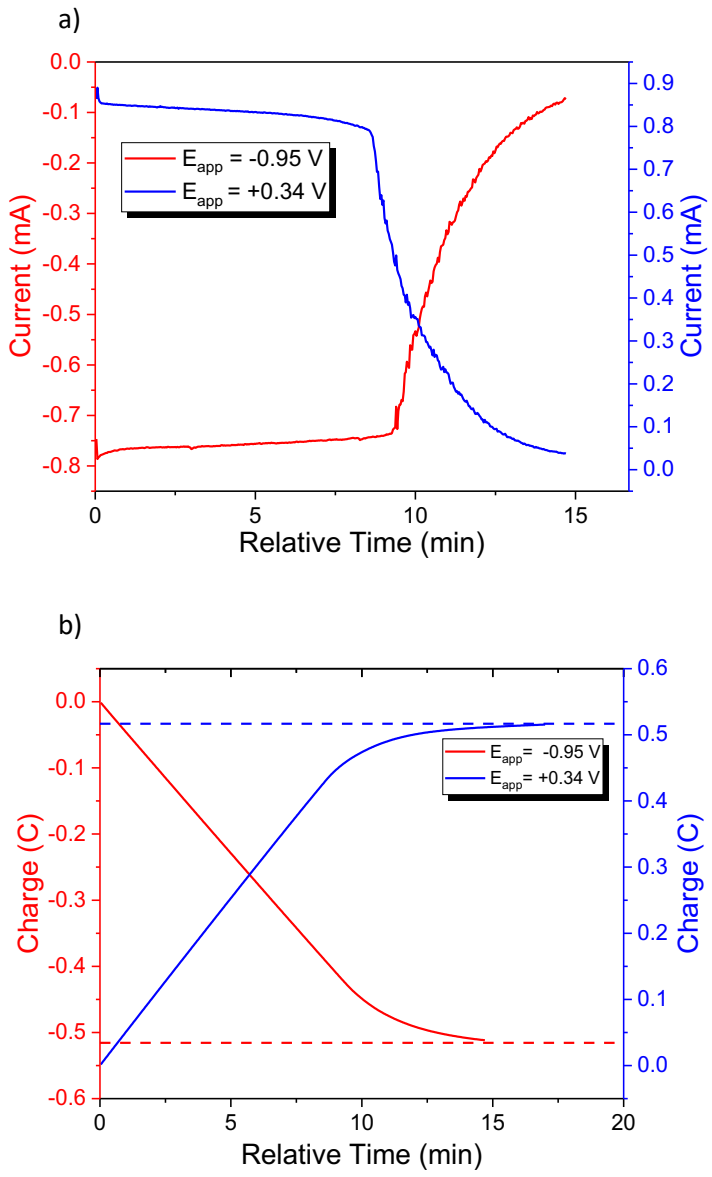

Figure S17 (a) Plots of current vs. relative time as recorded after applying a potential of -0.95 V (red) followed by +0.34 V (blue) to a solution containing **1** and before the addition of DDM (Figure S16). Note: the data shown under oxidizing conditions (blue) were recorded after the complex was reduced (red). The corresponding charge vs. relative time plots are shown in (b). Conditions: $[\mathbf{1}]_0$ = 0.5 mM, $[TBAPF_6]_0$ = 0.01 M, CH_2Cl_2.

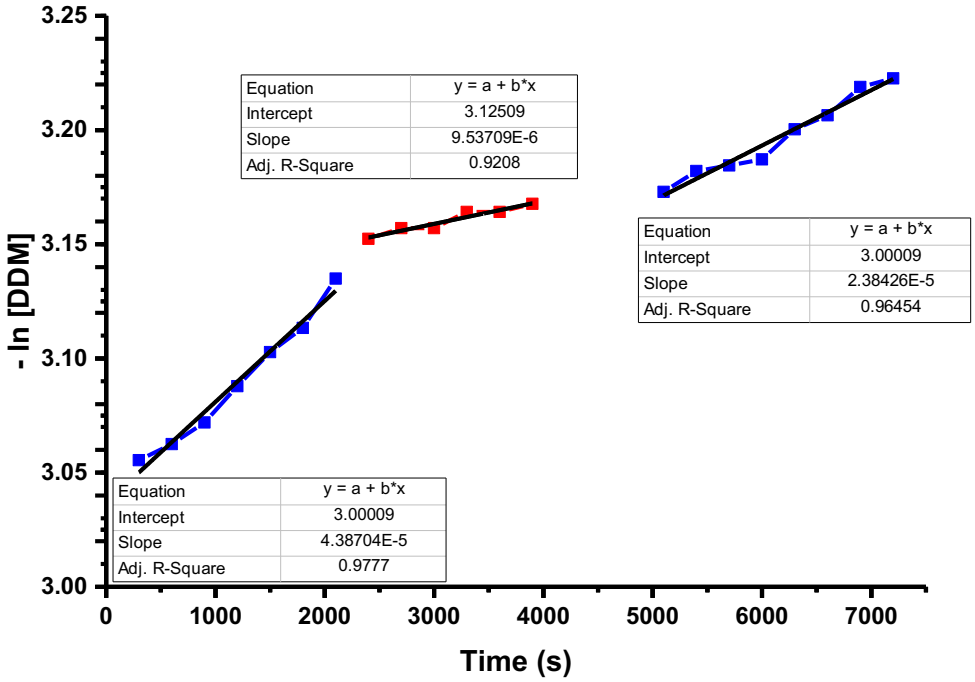

Figure S18 Plot of –ln [DDM] vs. time using **1** (■) as the catalyst. After initiating the reaction with **1**, a potential of -0.95 V was applied (■) followed by the subsequent application of a potential of +0.34 V (■) (Figure S19). Conditions: $[DDM]_0$ = 0.05 M, $[\mathbf{1}]_0$ = 0.5 mM, $[TBAPF_6]_0$ = 0.01 M, $[TMB]_0$ = 0.05 M, CH_2Cl_2.

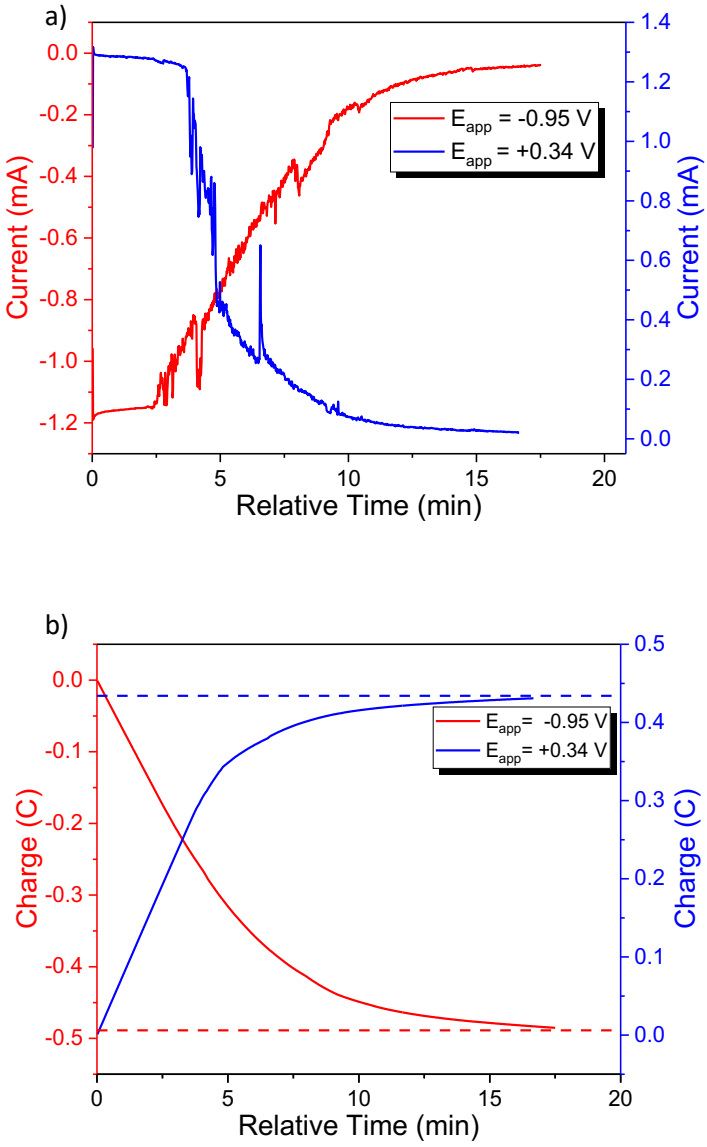

Figure S19 (a) Plots of current vs. relative time as recorded after applying a potential of -0.95 V (red) followed by +0.34 V (blue) to a solution containing **1** or $\mathbf{1}_{red}$ and DDM (Figure S18). Note: the data shown under oxidizing conditions (blue) were recorded 30 min after the complex was reduced (red). (b) Corresponding charge vs. relative time plots. Conditions: $[DDM]_0$ = 0.05 M, $[\mathbf{1}]_0$ = 0.5 mM, $[TBAPF_6]_0$ = 0.01 M, $[TMB]_0$ = 0.05 M, CH_2Cl_2.

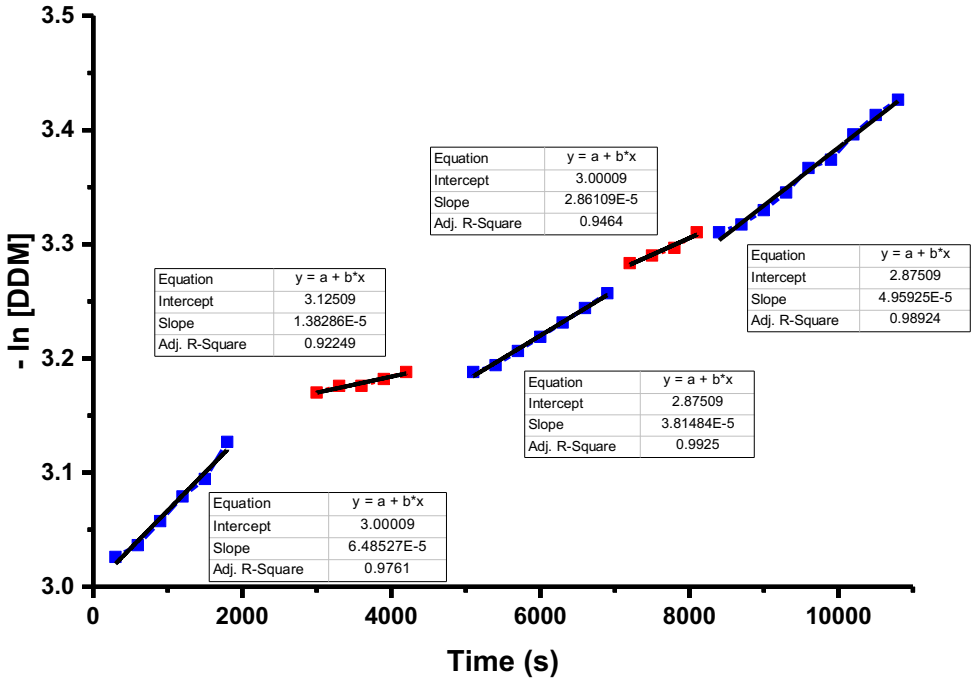

Figure S20 Plot of –ln [DDM] vs. time using **1** (■) as the catalyst. After initiating the reaction with **1**, a potential of -0.95 V was applied (■) followed by the subsequent application of a potential of +0.34 V (■) (Figure S21). Then, a potential of -0.95 V was applied (■) followed by a potential of +0.34 V (■) (Figure S22). Conditions: $[DDM]_0$ = 0.05 M, $[\mathbf{1}]_0$ = 0.5 mM, $[TBAPF_6]_0$ = 0.01 M, $[TMB]_0$ = 0.05 M, CH_2Cl_2.

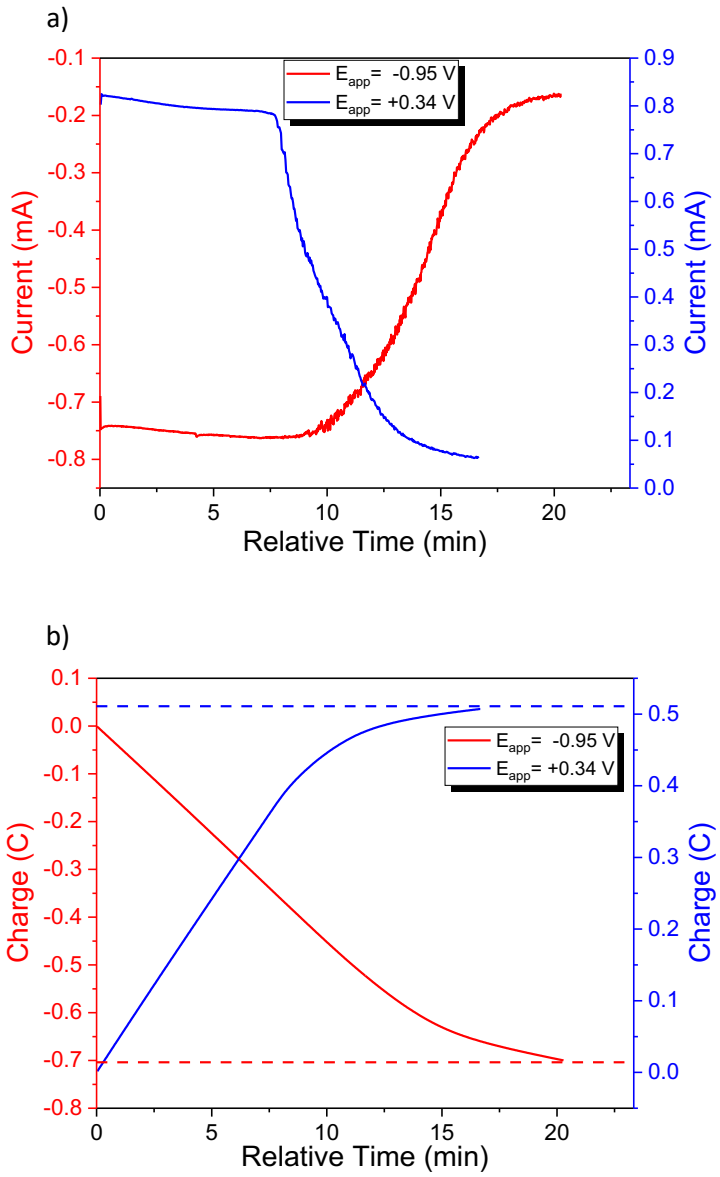

Figure S21 (a) Plots of current vs. relative time as recorded after applying a potential of -0.95 V (red) followed by +0.34 V (blue) to a solution containing **1** or $\mathbf{1}_{red}$ and DDM (Figure S20). Note: the data shown under oxidizing conditions (blue) were recorded 30 min after the complex was reduced (red). Note: the data shown under oxidizing conditions (blue) were recorded 30 min after the complex was reduced (red). (b) Corresponding charge vs. relative time plots. Conditions: $[DDM]_0 = 0.05$ M, $[\mathbf{1}]_0 = 0.5$ mM, $[TBAPF_6]_0 = 0.01$ M, $[TMB]_0 = 0.05$ M, CH_2Cl_2.

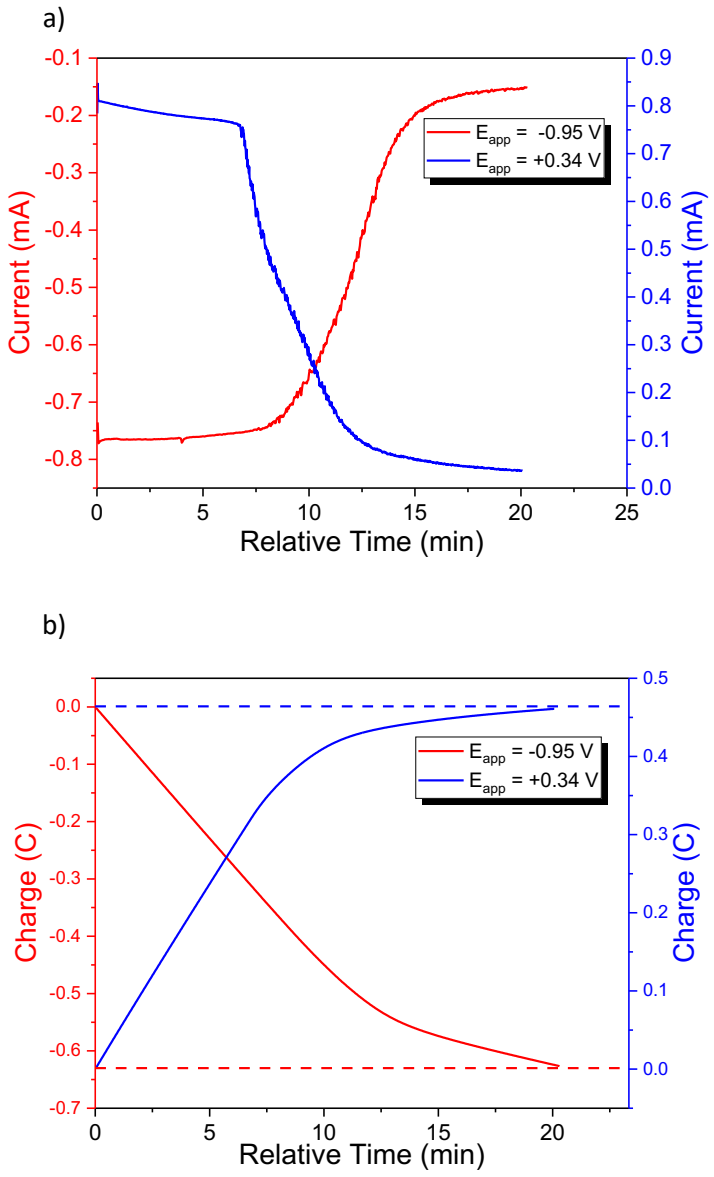

Figure S22 (a) Plots of current vs. relative time as recorded after applying a potential of -0.95 V (red) followed by +0.34 V (blue) to a solution containing **1** or $\mathbf{1}_{red}$ and DDM (Figure S20). Note: the data shown under oxidizing conditions (blue) were recorded 30 min after the complex was reduced (red). The corresponding charge vs. relative time plots are shown in (b). Conditions: $[DDM]_0 = 0.05$ M, $[\mathbf{1}]_0 = 0.5$ mM, $[TBAPF_6]_0 = 0.01$ M, $[TMB]_0 = 0.05$ M, CH_2Cl_2.

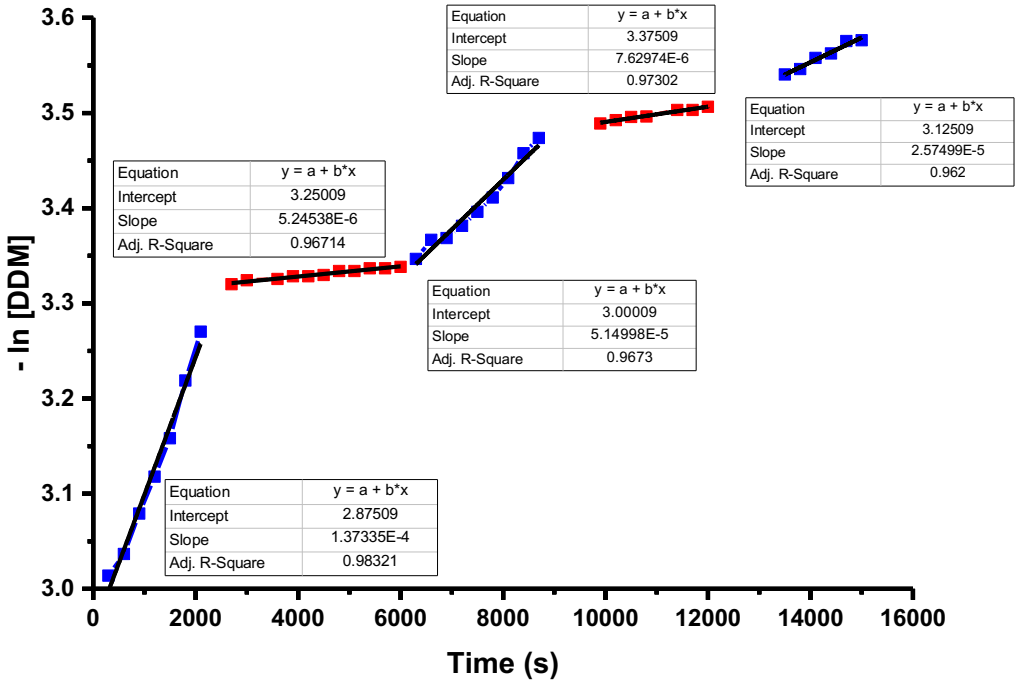

Figure S23 Plot of –ln [DDM] vs. time using **1** (■) as the catalyst. After initiating the reaction with **1**, a potential of -0.95 V was applied (■) followed by the subsequent application of a potential of +0.34 V (■) (Figure S24). Then, a potential of -0.95 V was applied (■) followed by a potential of +0.34 V (■) (Figure S25). Conditions: $[DDM]_0$ = 0.05 M, $[\mathbf{1}]_0$ = 0.5 mM, $[TBAPF_6]_0$ = 0.01 M, $[TMB]_0$ = 0.05 M, CH_2Cl_2.

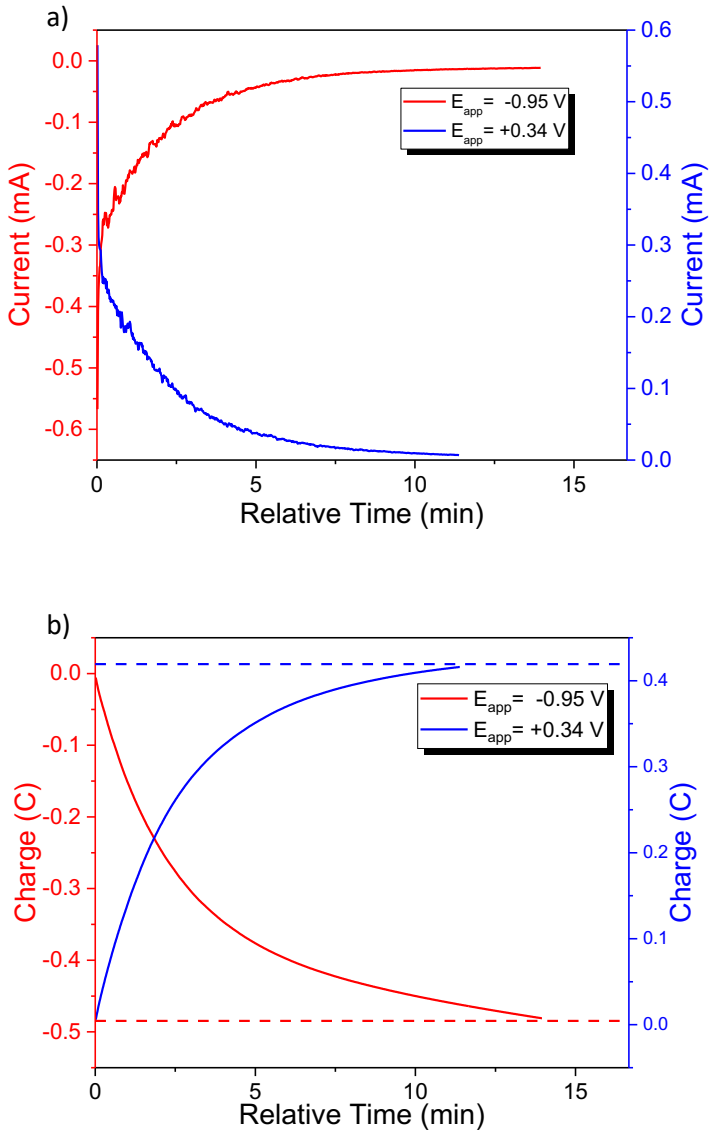

Figure S24 (a) Plots of current vs. relative time as recorded after applying a potential of -0.95 V (red) followed by +0.34 V (blue) to a solution containing **1** or $\mathbf{1}_{red}$ and DDM (Figure S23). Note: the data shown under oxidizing conditions (blue) were recorded 60 min after the complex was reduced (red). The corresponding charge vs. relative time plots are shown in (b). Conditions: $[DDM]_0 = 0.05$ M, $[\mathbf{1}]_0 = 0.5$ mM, $[TBAPF_6]_0 = 0.01$ M, $[TMB]_0 = 0.05$ M, CH_2Cl_2.

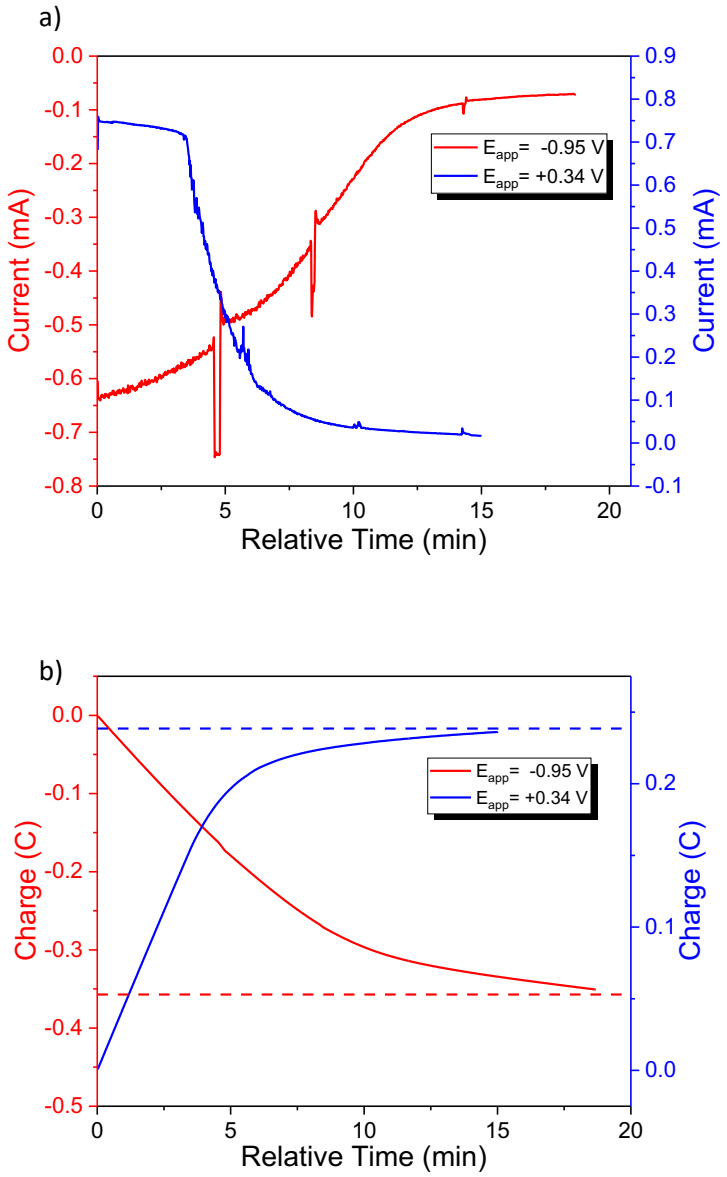

Figure S25 (a) Plots of current vs. relative time as recorded after applying a potential of -0.95 V (red) followed by +0.34 V (blue) to a solution containing **1** or $\mathbf{1}_{red}$ and DDM (Figure S23). Note: the data shown under oxidizing conditions (blue) were recorded 60 min after the complex was reduced (red). The corresponding charge vs. relative time plots are shown in (b). Conditions: $[DDM]_0 = 0.05$ M, $[\mathbf{1}]_0 = 0.5$ mM, $[TBAPF_6]_0 = 0.01$ M, $[TMB]_0 = 0.05$ M, CH_2Cl_2.

5. Potentiostatically-controlled ROMP data

a)

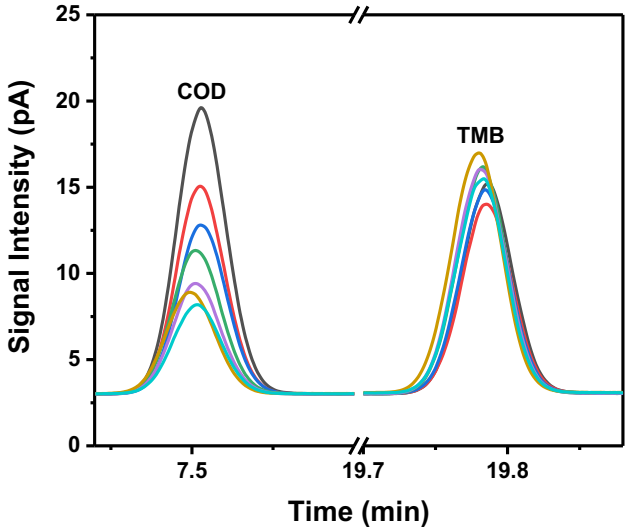

b)

t (min)	[COD]/[TMB]	Conv. (%)
0	1.18	0
10	0.94	20.3
20	0.73	38.1
30	0.56	52.5
40	0.41	65.3
50	0.31	73.7
60	0.22	81.4

c)

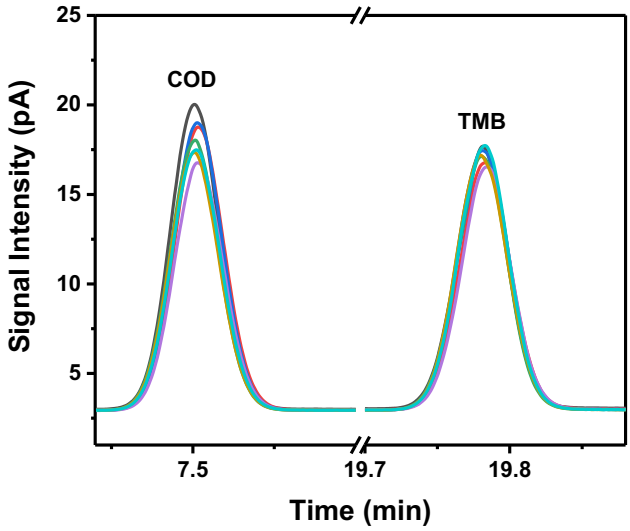

d)

t (min)	[COD]/[TMB]	Conv. (%)
0	1.18	0
10	1.02	13.6
20	0.98	16.9
30	0.96	18.6
40	0.91	22.9
50	0.89	24.6
60	0.85	28.0

Figure S26 (a) Representative GC data recorded over time for the ROMP of COD using **1** as the initiator. (b) Summary of the signal integral ratios for the data shown in panel (a) and corresponding substrate conversions as a function of time. (c) Representative GC data recorded over time for the ROMP of COD using $\mathbf{1}_{red}$ as the initiator. (d) Summary of the signal integral ratios for the data shown in panel (c) and corresponding substrate conversions as a function of time. Conditions: $[COD]_0$ = 0.05 M, $[\mathbf{1}]_0$ or $[\mathbf{1}_{red}]_0$ = 0.5 mM, $[TBAPF_6]_0$ = 0.01 M, $[TMB]_0$ = 0.05 M, CH_2Cl_2.

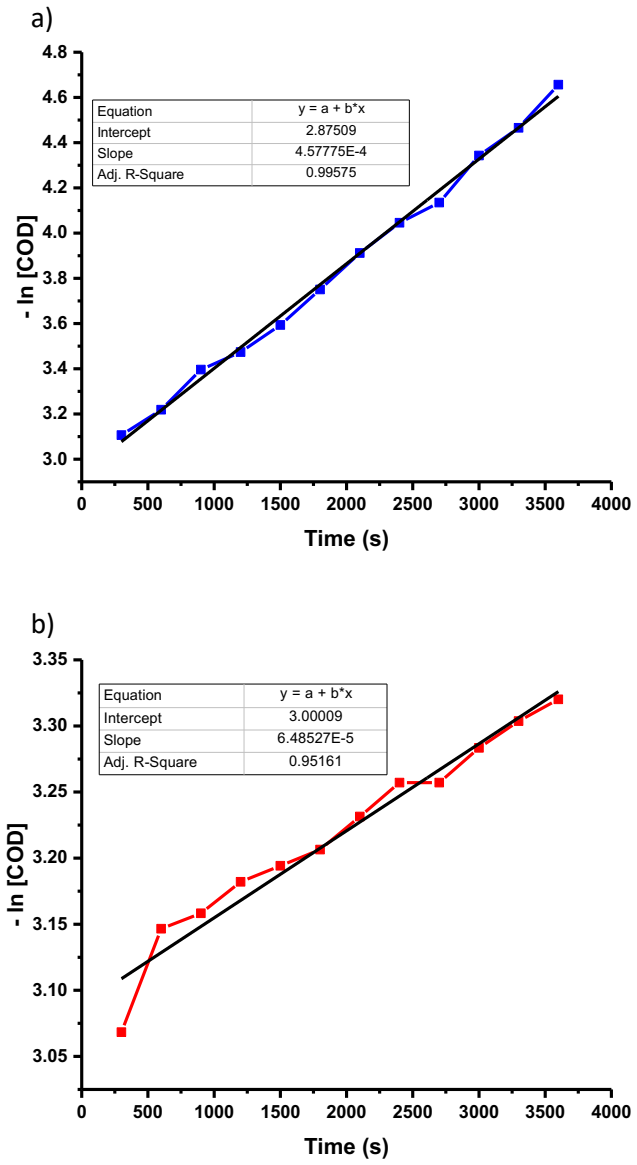

Figure S27 (a) Plot of –ln [COD] vs. time using **1** (■) as the initiator. (b) Plot of –ln [COD] vs time using $\mathbf{1_{red}}$ **(■)** as the initiator (Figure S28). Conditions: $[COD]_0 = 0.05$ M, $[\mathbf{1}]_0$ or $[\mathbf{1_{red}}]_0 = 0.5$ mM, $[TBAPF_6]_0 = 0.01$ M, $[TMB]_0 = 0.05$ M, CH_2Cl_2.

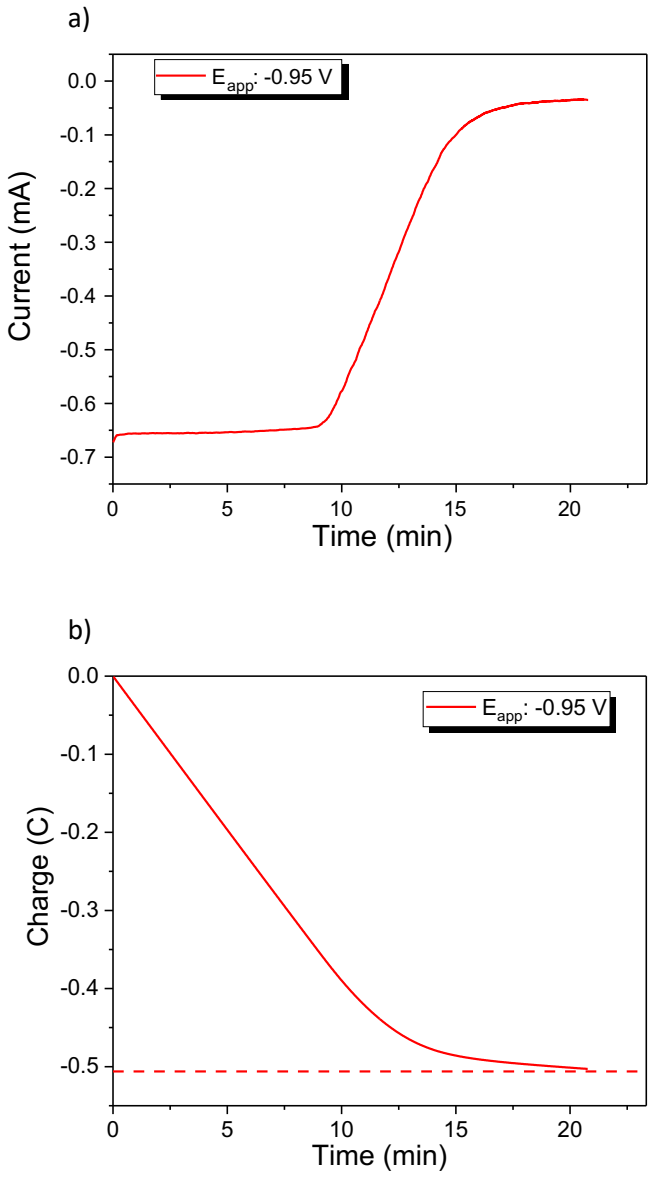

Figure S28 (a) Plot of current vs. time as recorded after applying a potential of -0.95 V to a solution of **1** and before the addition of COD (Figure 27b). (b) Corresponding charge vs. time plot. Conditions: $[\mathbf{1}]_0$ = 0.5 mM, $[TBAPF_6]_0$ = 0.01 M, CH_2Cl_2.

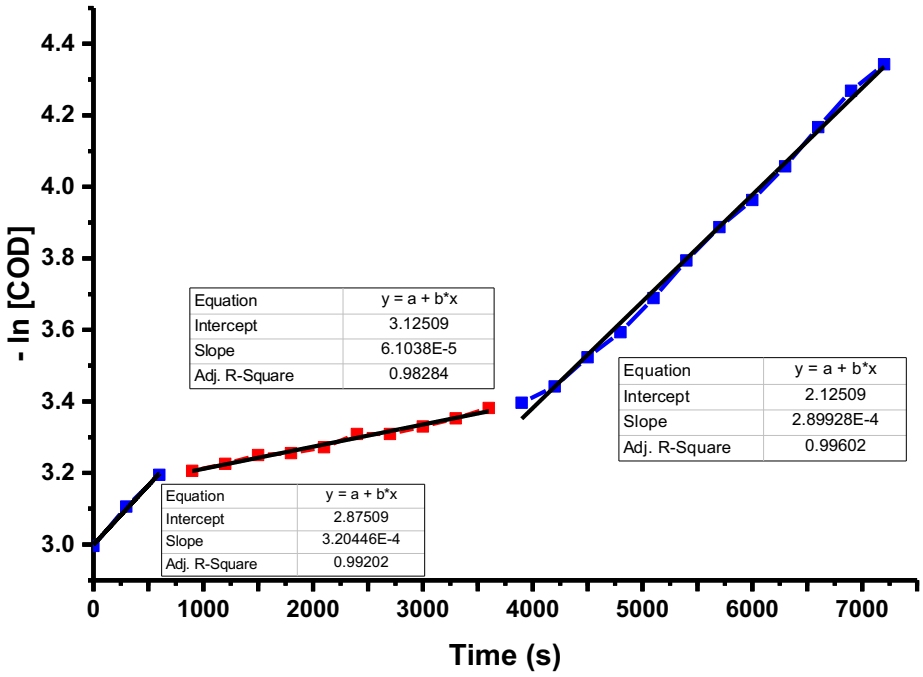

Figure S29 Plot of –ln $[COD]_0$ vs. time using **1** (■) as the initiator. After initiating the reaction with **1**, a potential of -0.95 V was applied (■) followed by the subsequent application of a potential of +0.34 V (■) (Figure S30). Conditions: $[COD]_0$ = 0.05 M, $[\mathbf{1}]_0$ = 0.5 mM, $[TBAPF_6]_0$ = 0.01 M, $[TMB]_0$ = 0.05 M, CH_2Cl_2.

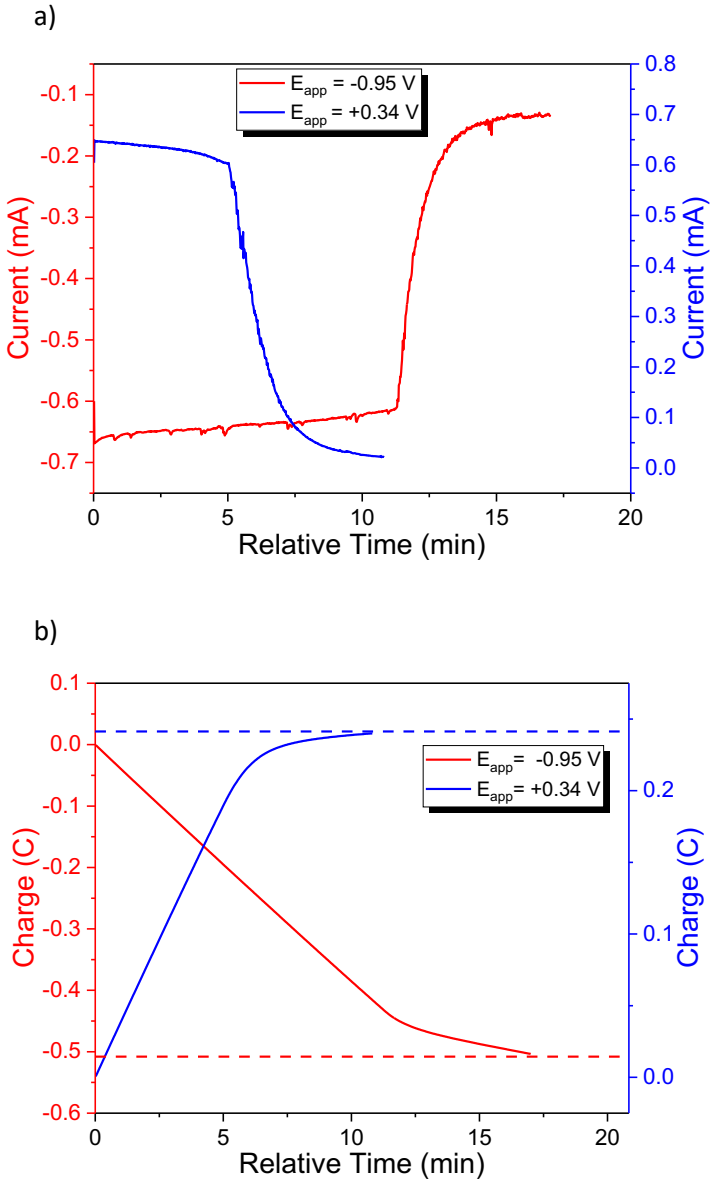

Figure S30 (a) Plots of current vs. relative time as recorded after applying a potential of -0.95 V (red) followed by +0.34 V (blue) to a solution containing **1** or $\mathbf{1}_{red}$ and COD (Figure S29). Note: the data shown under oxidizing conditions (blue) were recorded 30 min after the complex was reduced (red). The corresponding charge vs. relative time plots are shown in (b). Conditions: $[COD]_0 = 0.05$ M, $[\mathbf{1}]_0 = 0.5$ mM, $[TBAPF_6]_0 = 0.01$ M, $[TMB]_0 = 0.05$ M, CH_2Cl_2.

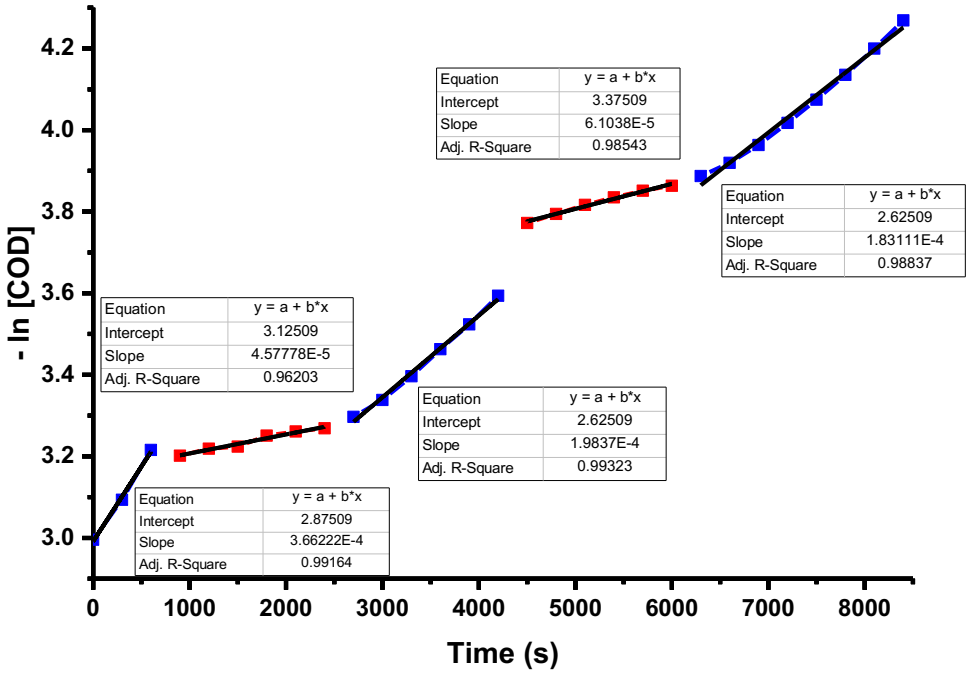

Figure S31 Plot of –ln [COD] vs. time using **1** (■) as the initiator. After initiating the reaction with **1**, a potential of -0.95 V was applied (■) followed by the subsequent application of a potential of +0.34 V (■) (Figure S32). Then, a potential of -0.95 V was applied (■) followed by a potential of +0.34 V (■) (Figure S33). Conditions: $[COD]_0$ = 0.05 M, $[\mathbf{1}]_0$ = 0.5 mM, $[TBAPF_6]_0$ = 0.01 M, $[TMB]_0$ = 0.05 M, CH_2Cl_2.

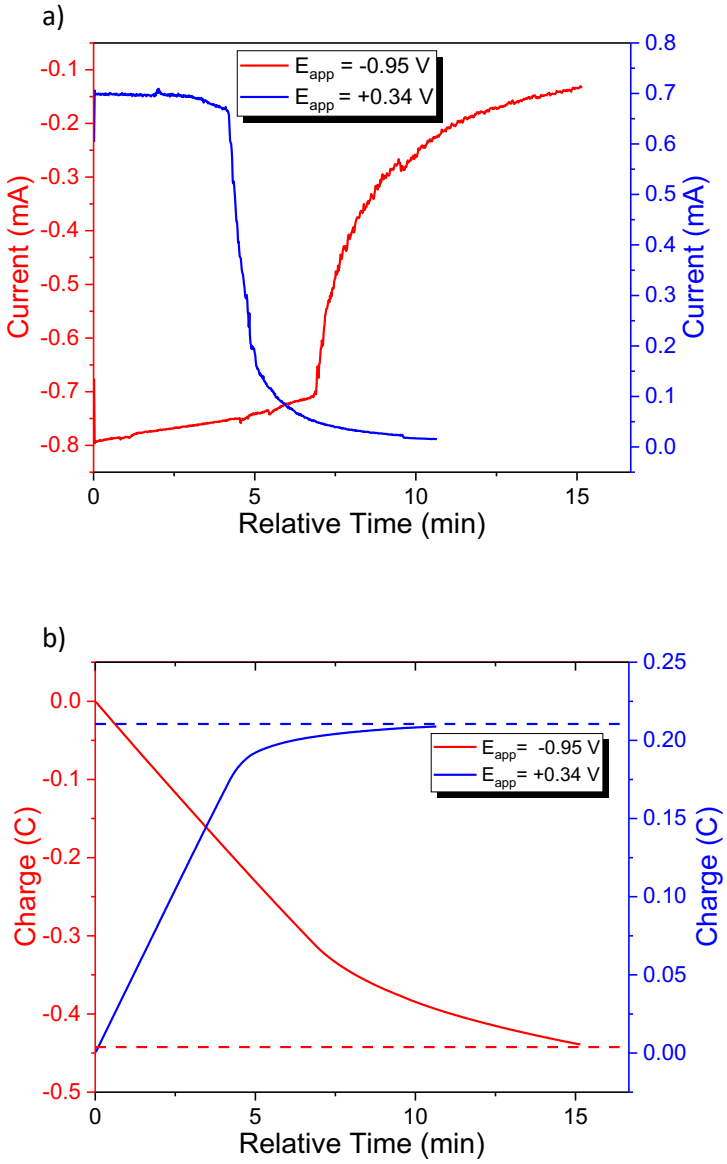

Figure S32 (a) Plots of current vs. relative time as recorded after by applying a potential of -0.95 V (red) followed by +0.34 V (blue) to a solution containing **1** or $\mathbf{1}_{red}$ and COD (Figure S31). Note: the data shown under oxidizing conditions (blue) were recorded 30 min after the complex was reduced (red). The corresponding charge vs. relative time plots are shown in (b). Conditions: $[COD]_0 = 0.05$ M, $[\mathbf{1}]_0 = 0.5$ mM, $[TBAPF_6]_0 = 0.01$ M, $[TMB]_0 = 0.05$ M, CH_2Cl_2.

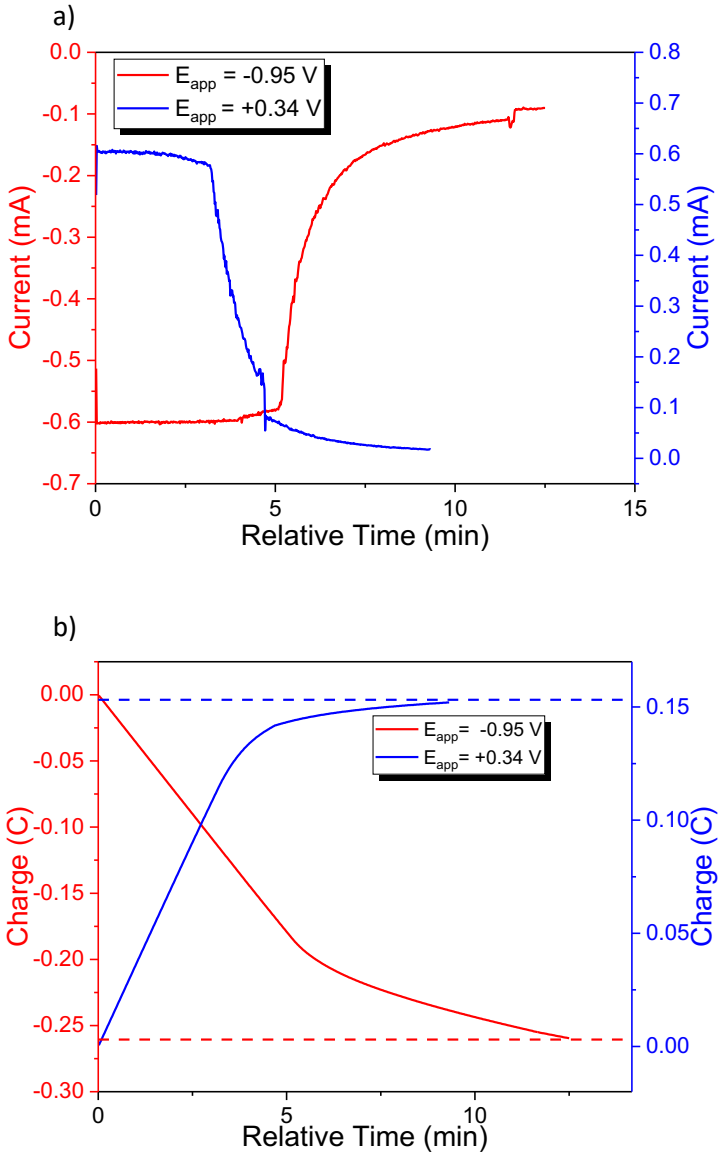

Figure S33 (a) Plots of current vs. relative time as recorded after applying a potential of -0.95 V (red) followed by +0.34 V (blue) to a solution containing **1** or $\mathbf{1}_{red}$ and COD (Figure S31). Note: the data shown under oxidizing conditions (blue) were recorded 30 min after the complex was reduced (red). The corresponding charge vs. relative time plots are shown in (b). Conditions: $[COD]_0$ = 0.05 M, $[\mathbf{1}]_0$ = 0.5 mM, $[TBAPF_6]_0$ = 0.01 M, $[TMB]_0$ = 0.05 M, CH_2Cl_2.

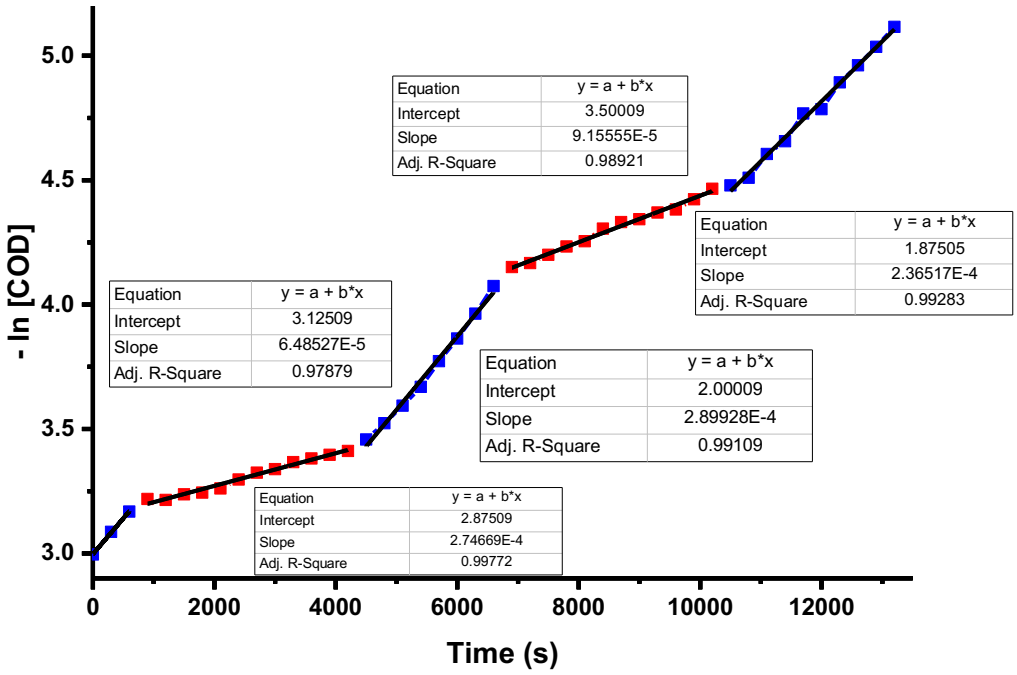

Figure S34 Plot of –ln [COD] vs. time using **1** (■) as the initiator. After initiating the reaction with **1**, a potential of -0.95 V was applied (■) followed by the subsequent application of a potential of +0.34 V (■) (Figure S35). Then, a potential of -0.95 V was applied (■) followed by a potential of +0.34 V (■) (Figure S36). Conditions: $[COD]_0$ = 0.05 M, $[\mathbf{1}]_0$ = 0.5 mM, $[TBAPF_6]_0$ = 0.01 M, $[TMB]_0$ = 0.05 M, CH_2Cl_2.

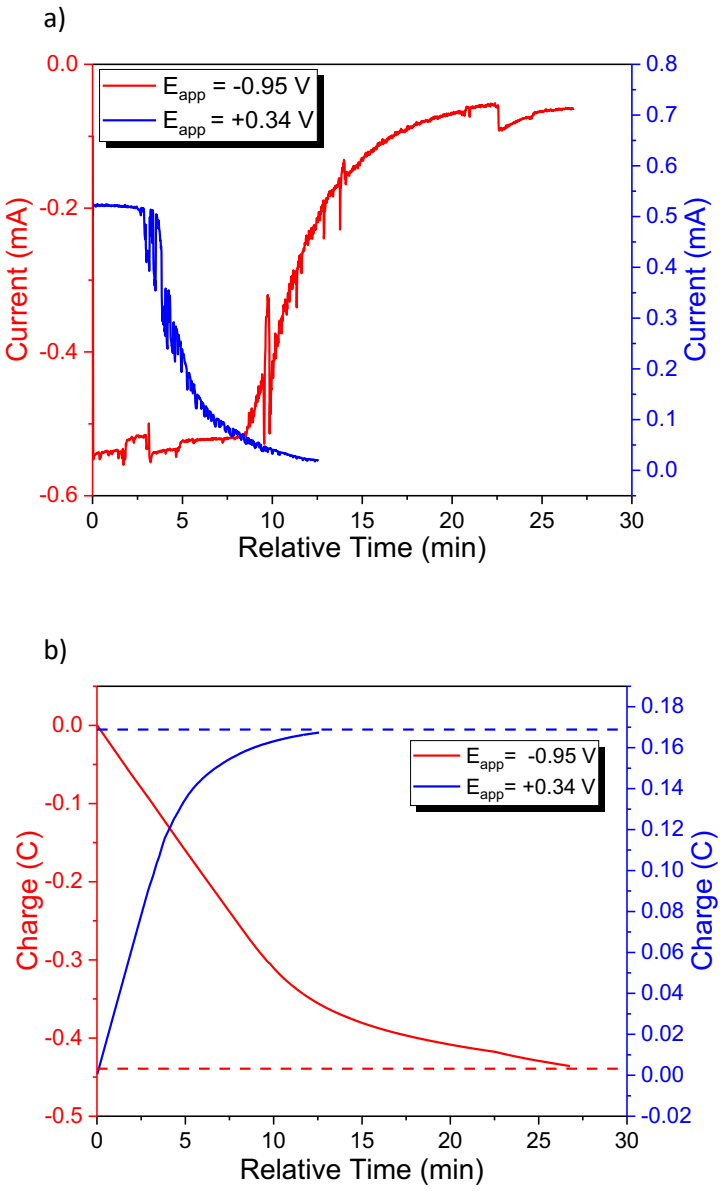

Figure S35 (a) Plots of current vs. relative time as recorded after applying a potential of -0.95 V (red) followed by +0.34 V (blue) to a solution containing **1** or $\mathbf{1}_{red}$ and COD (Figure S34). Note: the data shown under oxidizing conditions (blue) were recorded 60 min after the complex was reduced (red). The corresponding charge vs. relative time plots are shown in (b). Conditions: $[COD]_0$ = 0.05 M, $[\mathbf{1}]_0$ = 0.5 mM, $[TBAPF_6]_0$ = 0.01 M, $[TMB]_0$ = 0.05 M, CH_2Cl_2.

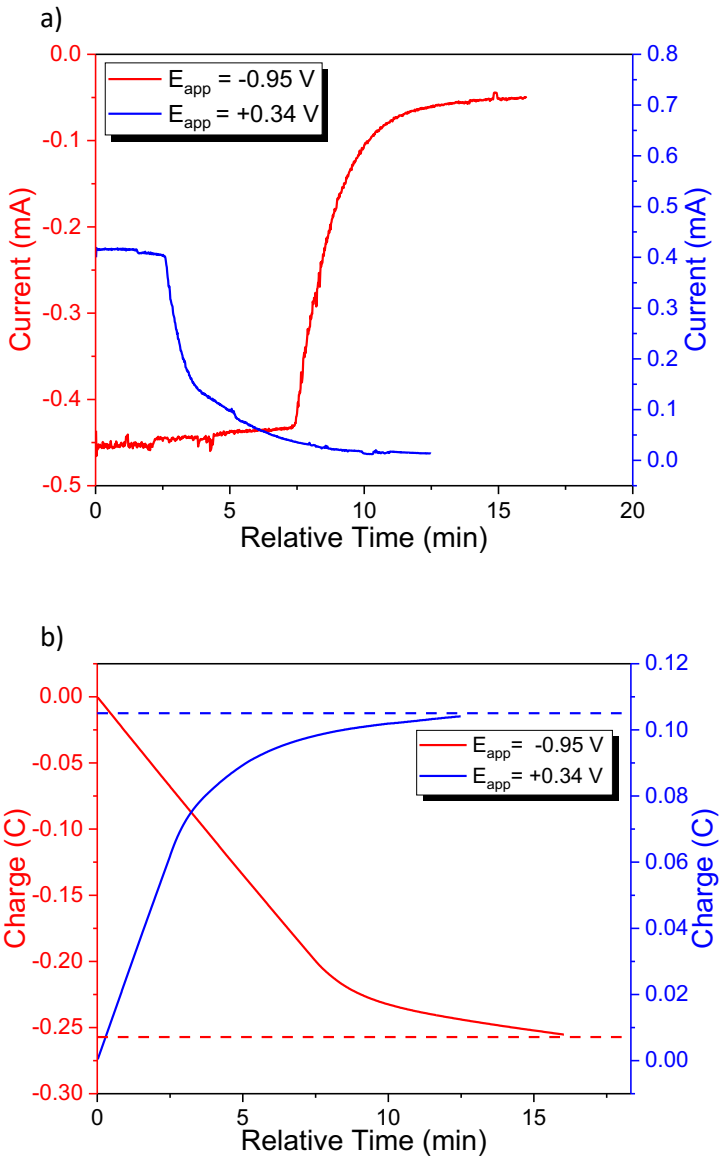

Figure S36 (a) Plot of current vs. relative time as recorded after applying a potential of -0.95 V (red) followed by +0.34 V (blue) to a solution containing **1** or $\mathbf{1}_{red}$ and COD (Figure S34). Note: the data shown under oxidizing conditions (blue) were recorded 60 min after the complex was reduced (red). The corresponding charge vs. relative time plots are shown in (b). Conditions: $[COD]_0$ = 0.05 M, $[\mathbf{1}]_0$ = 0.5 mM, $[TBAPF_6]_0$ = 0.01 M, $[TMB]_0$ = 0.05 M, CH_2Cl_2.

6. Polymer characterization data

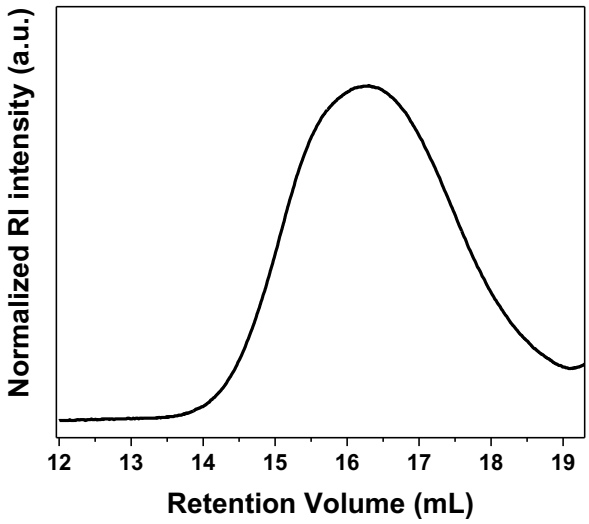

Figure S37 Size exclusion chromatogram recorded of the crude mixture that was obtained after COD was polymerized using **1** as the initiator and conducted in the absence of an applied potential. Conditions and data: $[COD]_0$ = 0.05 M, $[\mathbf{1}]_0$ = 0.5 mM, $[TMB]_0$ = 0.05 M, $[TBAPF_6]_0$ = 0.01 M, CH_2Cl_2; M_n = 25.6 kDa, Đ = 2.20; conversion of monomer to polymer = 81%; isolated yield = 77%.

a)

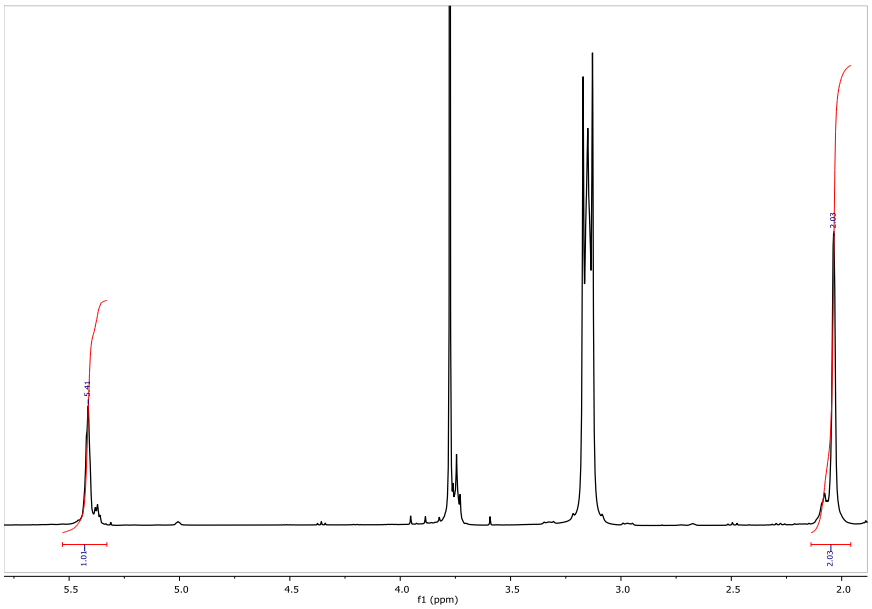

b)

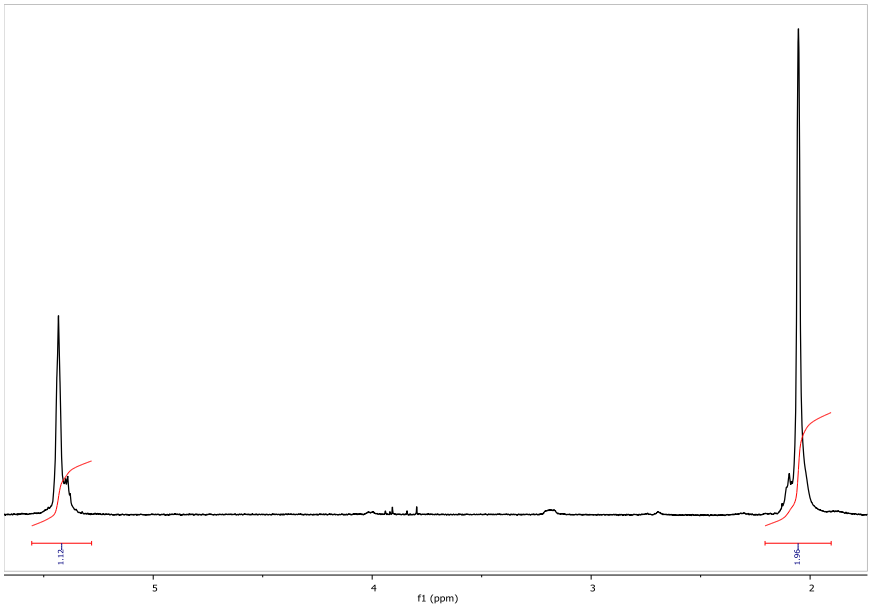

Figure S38 (a) ^{1}H NMR spectrum recorded of the crude mixture that was obtained after COD was polymerized using **1** as the initiator and conducted in the absence of an applied potential. The mixture was first dried in a vacuum and then dissolved in $CDCl_3$ prior to analysis. Note: the signals observed at δ 3.8 and 3.2 ppm were assigned to TMB and $TBAPF_6$, respectively. (b) ^{1}H NMR spectrum recorded after the polymer was purified by pouring the reaction mixture into methanol to induce precipitation. Conditions: $[COD]_0$ = 0.05 M, $[\mathbf{1}]_0$ = 0.5 mM, $[TMB]_0$ = 0.05 M, $[TBAPF_6]_0$ = 0.01 M, CH_2Cl_2; conversion of monomer to polymer = 81%; isolated yield = 77%.

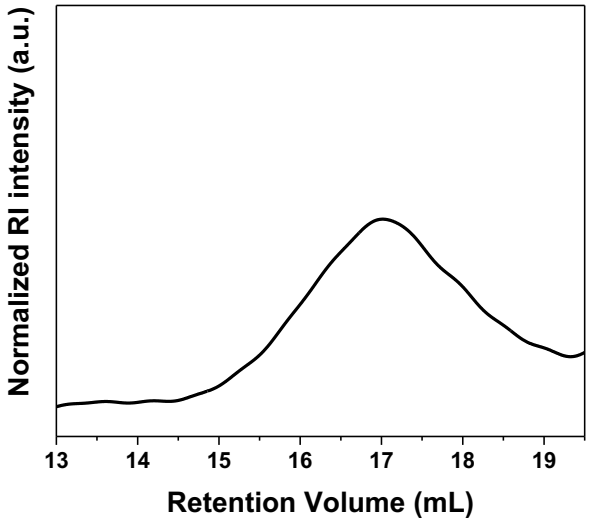

Figure S39 Size exclusion chromatogram recorded of crude reaction mixture that was obtained after COD was polymerized using **1** and conducted under an applied potential (see main text). Conditions and data: $[COD]_0$ = 0.05 M, $[\mathbf{1}]_0$ = 0.5 mM, $[TMB]_0$ = 0.05 M, $[TBAPF_6]_0$ = 0.01 M, CH_2Cl_2; M_n = 13.1 kDa, Đ = 2.24; conversion of monomer to polymer = 22%.

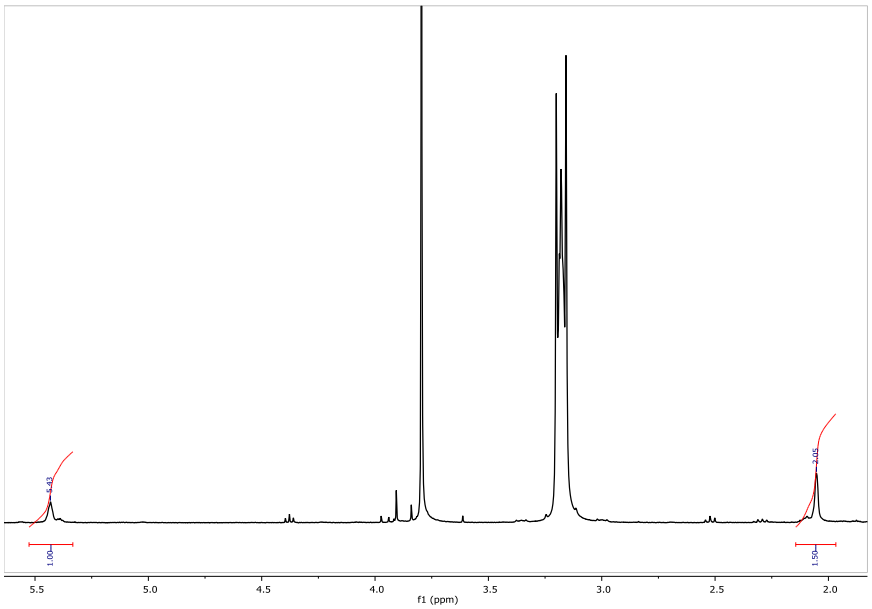

Figure S40 ^{1}H NMR spectrum recorded of the crude reaction mixture that was obtained after COD was polymerized using **1** as the initiator and conducted under an applied potential (see main text). The aliquot mixture was first dried in a vacuum and then dissolved in $CDCl_3$ prior to analysis. Note: the signals observed at δ 3.8 and 3.2 ppm were assigned to TMB and $TBAPF_6$, respectively. Conditions and data: $[COD]_0$ = 0.05 M, $[\mathbf{1}]_0$ = 0.5 mM, $[TMB]_0$ = 0.05 M, $[TBAPF_6]_0$ = 0.01 M, CH_2Cl_2, conversion of monomer to polymer = 22%.

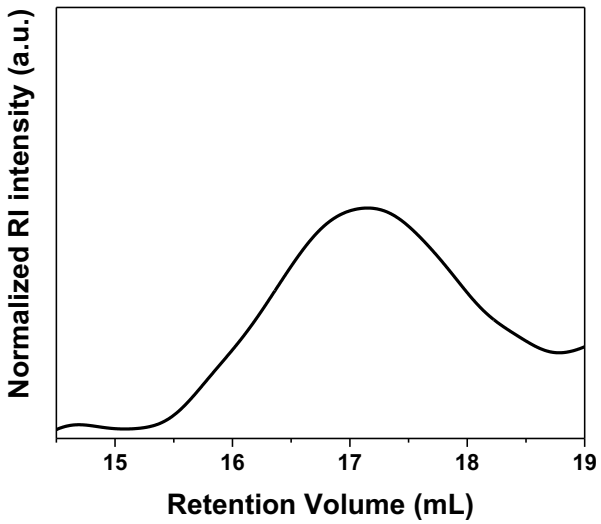

Figure S41 Size exclusion chromatogram recorded of crude reaction mixture that was obtained after COD was polymerized using **1** and conducted under an applied potential (see main text). Conditions and data: $[COD]_0$ = 0.05 M, $[\mathbf{1}]_0$ = 0.5 mM, $[TMB]_0$ = 0.05 M, $[TBAPF_6]_0$ = 0.01 M, CH_2Cl_2; M_n = 16.7 kDa, Đ = 2.3; conversion of monomer to polymer = 29%.

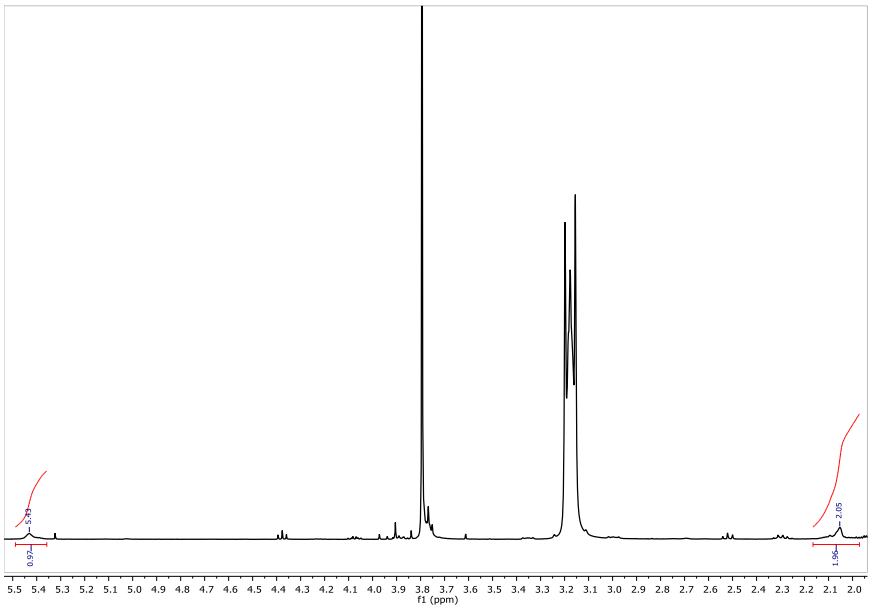

Figure S42 ^{1}H NMR spectrum recorded of the crude reaction mixture that was obtained after COD was polymerized using **1** as the initiator and conducted under an applied potential (see main text). The mixture was first dried in a vacuum and then dissolved in $CDCl_3$ prior to analysis. Note: the signals observed at δ 3.8 and 3.2 ppm were assigned to TMB and $TBAPF_6$, respectively. Conditions and data: $[COD]_0$ = 0.05 M, $[\mathbf{1}]_0$ = 0.5 mM, $[TMB]_0$ = 0.05 M, $[TBAPF_6]_0$ = 0.01 M, CH_2Cl_2; conversion of monomer to polymer = 29%.

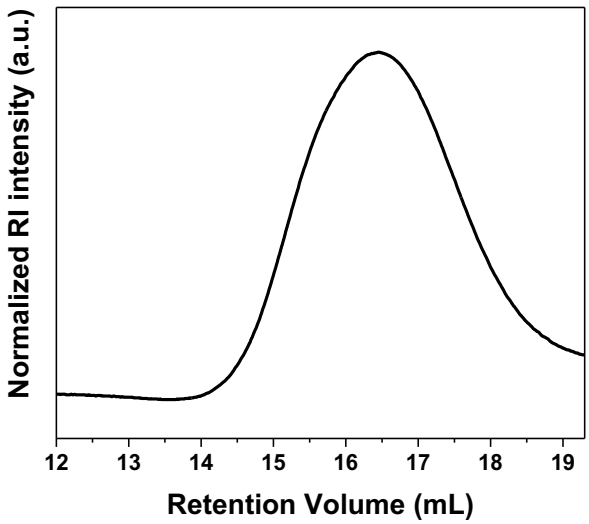

Figure S43 Size exclusion chromatogram recorded of the crude mixture that was obtained after COD was polymerized using **1** and conducted under an applied potential (see main text). Conditions and data: $[COD]_0$ = 0.05 M, $[\mathbf{1}]_0$ = 0.5 mM, $[TMB]_0$ = 0.05 M, $[TBAPF_6]_0$ = 0.01 M, CH_2Cl_2; M_n = 23.4 kDa, Đ = 2.17; conversion of monomer to polymer = 80%, isolated yield = 75%.

a)

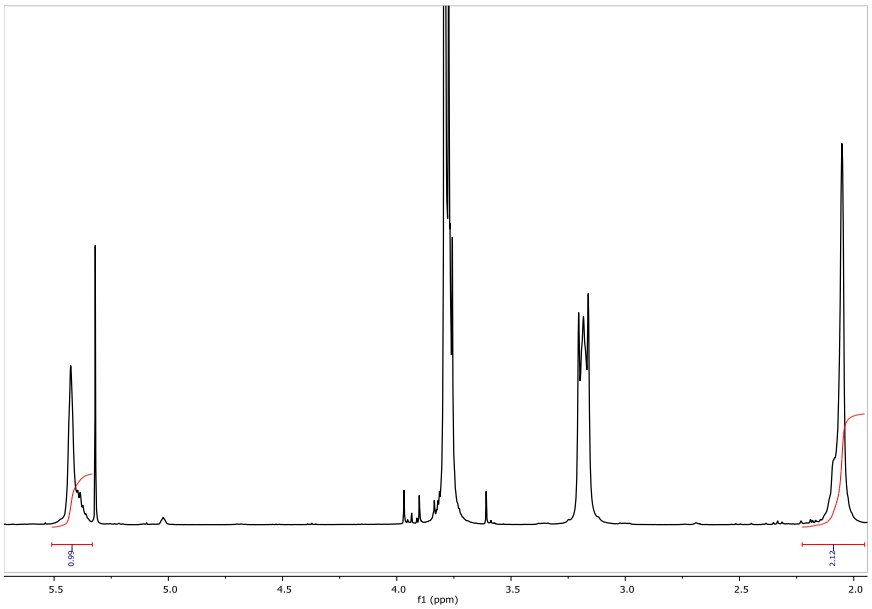

b)

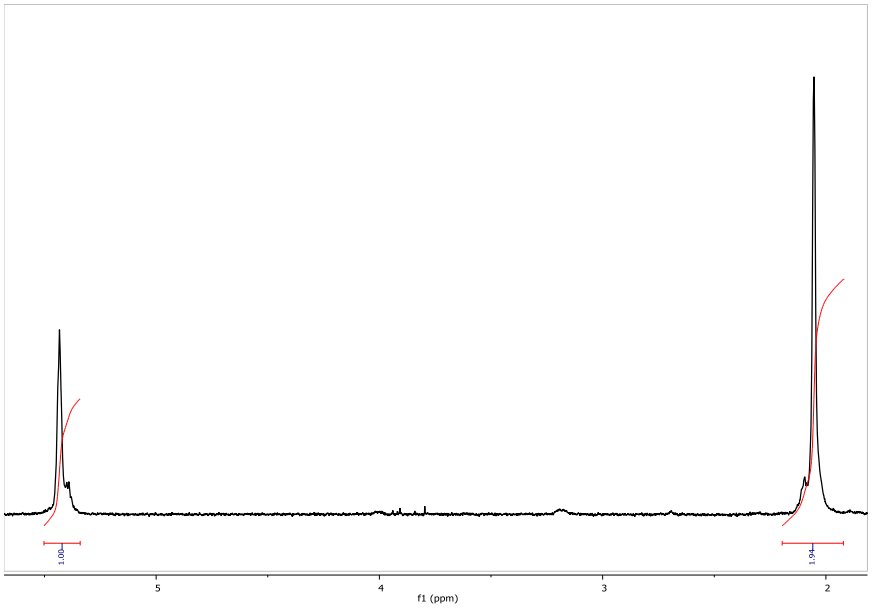

Figure S44 (a) ^{1}H NMR spectrum recorded of the crude mixture that was obtained after COD was polymerized using **1** as the initiator and conducted under an applied potential (see main text). The mixture was first dried in a vacuum and then dissolved in $CDCl_3$ prior to analysis. Note: the signals observed at δ 3.8 and 3.2 ppm were assigned to TMB and $TBAPF_6$, respectively. (b) ^{1}H NMR spectrum recorded after the polymer was purified by pouring the mixture into methanol to induce precipitation. Conditions and data: $[COD]_0 = 0.05$ M, $[\mathbf{1}]_0 = 0.5$ mM, $[TMB]_0 = 0.05$ M, $[TBAPF_6]_0 = 0.01$ M, CH_2Cl_2; conversion of monomer to polymer = 80%, isolated yield = 75%.

7. References

(1) Lastovickova, D. N.; Teator, A. J.; Shao, H.; Liu, P.; Bielawski, C. W. A Redox-Switchable Ring-Closing Metathesis Catalyst. *Inorg. Chem. Front.* **2017**, *4* (9), 1525–1532.

(2) Connelly, N. G.; Geiger, W. E. Chemical Redox Agents for Organometallic Chemistry. *Chem. Rev.* **1996**, *96* (2), 877–910.